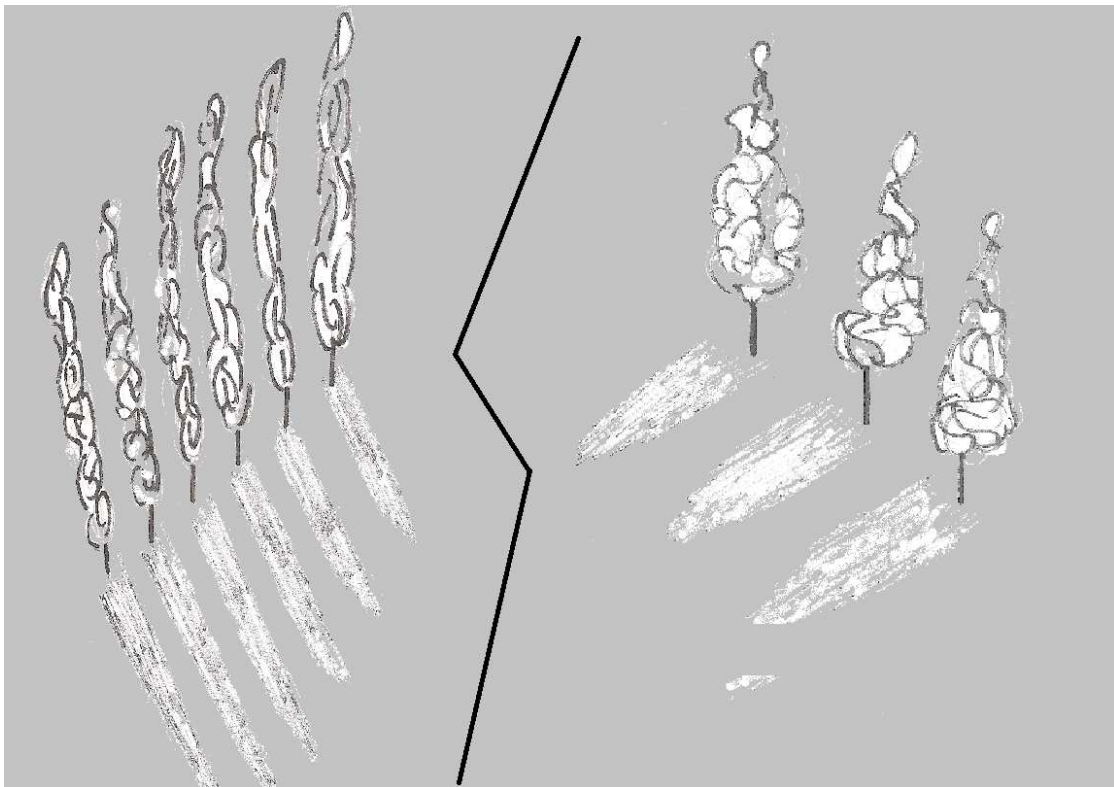# Tree Spacing of Spindle- versus Columnar Apple Tree Orchard Systems;

Measuring and modelling light interception and fruit production efficiency

H.L. van de Graaf

MSc student Crop Sciences

MSc thesis Plant Production Systems

April, 2010

Tree Spacing of Spindle- versus Columnar Apple Tree Orchard Systems;

Measuring and modelling light interception and fruit production efficiency

H.L. van de Graaf

MSc student Crop Sciences

Registration number: 860117-274-120

PPS-80436 Thesis Plant Production Systems

April 2010

Supervisors: Dr. Ir. P.A. Leffelaar

Plant Production Systems Group

Dr. Ir. E. Heuvelink

Horticultural Supply Chains Group

Dr. F.M. Maas

Applied Plant Research; Fruit

Examiner: Dr. N. de Ridder

WAGENINGEN UNIVERSITY
WAGENINGEN UR

TABLE OF CONTENTS

PREFACE

This report was written in the context of the course PPS-80436 Thesis Plant Production Systems. The aim of this course is familiarization with all different aspects which play a role in setting up and conducting a thesis research.

This project was carried out in the Plant Production Systems group in combination with the Horticultural Supply Chains group and Applied Plant Research (fruit) of Wageningen University and Research Centre. These parties were represented by Dr. ir. Peter Leffelaar, Dr. ir. Ep Heuvelink and Dr. Frank Maas, respectively, who supervised this project.

Throughout my MSc thesis I gained more insight and experience in conducting experiments, data analysis, modelling and drawing scientifically valid conclusions. Furthermore, I got acquainted with the working atmosphere in a research station; Applied Plant Research for fruit. The challenge of this thesis for me was to be responsible for both planning and carrying out a scientific experiment, as well as using the obtained data in a mathematically underpinned model.

I would like to thank all supervisors involved for their help and dedication during my thesis research. Furthermore, Aad van der Heide was so kind to allow me to conduct measurements at his columnar apple trees, for which I would like to thank him. Finally, I would like to mention my appreciation to Prof.dr.ir. Jan Goudriaan for giving me feedback on the theoretical part on light interception in row crop canopies.

SUMMARY

The Columnar Apple Tree System (CATS) combines columnar growth with higher tree densities compared to the spindle apple tree system. The former system is not yet commercially introduced, but it potentially could achieve higher fruit yields per ha compared to the currently used spindle tree apple orchard system. The most important reason for this is that the columnar shape allows for a better, more evenly distributed light interception. Still, light interception is influenced by tree spacing. Furthermore, in order to achieve high fruit yields, the intercepted light should be efficiently used to produce fruit.

This study aims to obtain the optimal plant spacing of columnar- versus spindle apple tree systems by measuring and modelling their light interception and fruit production efficiency (dry weight yield per unit of photosynthetic active radiation intercepted). Optimal plant spacing is defined as the plant spacing at which 70% of the available amount of PAR is intercepted by the canopy, since higher interception values were previously found to decrease fruit quality (especially fruit colouration) by increasing internal canopy shading.

From bloom till directly after harvest (for the columnar as well as the spindle apple trees) monthly light measurements were taken using the SunScan Canopy Analysis System underneath and within the canopy at different times during the day and two sides of the orchard row. Furthermore, leaf area index and fruit weight (fresh and dry) were measured monthly, whereas fruit colour of both tree types was determined only at harvest.

The optimal plant spacing was found to be rectangular for both apple tree systems (0.80x0.80m for the SATS and 0.3x0.3m for the CATS) according to the model ROWCROP, which resulted in a fraction PAR intercepted of 0.46 and 0.41 for the SATS and the CATS respectively (compared to 0.38 and 0.34 when using the default tree spacing (path width of 3.25 and 2.50m and row width of 0.80 and 0.30m for the SATS and the CATS respectively). However this tree spacing is not realistic considering the size of the machinery currently used in the orchards; the path width should be minimally 2.00m in order to allow this machinery to drive through. According to ROWCROP using this more realistic tree spacing (2.00x2.00m) the fraction PAR intercepted becomes 0.40 and 0.36 for the SATS and the CATS respectively. Assuming that the LAI increases linearly with the tree height, the 70% PAR interception aimed at could only be achieved at 5.00m tree height using the optimal plant spacing for both apple tree systems (path width of 0.80 and 0.3m and row width of 0.80 and 0.3m for the SATS and the CATS respectively).

The apple production efficiency was higher for the SATS than the CATS over time.

1. INTRODUCTION

From the early 18th century until now, Dutch apple planting systems evolved from 'fruit meadows' with large, widely spaced high apple trees interplanted with other fruit trees, into specialized systems with small, slender trees planted at high densities (Balkhoven-Baart *et al.*, 2000; Wagenmakers, 1991; Wagenmakers, 1995a). The advantages of this intensification involve early bearing, lower labour costs due to lower trees, reduced pesticide use and a higher proportion and more even distribution of high, good quality, fruit yields (Balkhoven-Baart *et al.*, 2000; Tromp *et al.*, 2005; Wagenmakers, 1995b). Consequently, relatively early renewal of the orchard became feasible. The latter enabled the grower to benefit early from yield improving developments like new cultivars, rootstocks or planting systems (Balkhoven-Baart *et al.*, 2000; Tromp *et al.*, 2005; Wagenmakers, 1991; Wagenmakers, 1995a).

In the Netherlands apple orchards are currently planted in single rows, with planting distances varying from 3.00 x 0.75 to 3.00 x 1.25 m using thin slender spindle trees (Balkhoven-Baart *et al.*, 2000). Planting densities varying between 3000 and 6000 trees per ha are considered to be economically optimal (Balkhoven-Baart *et al.*, 2000).

The Columnar Apple Tree System (CATS) is an apple planting system that is not yet introduced in the Netherlands, which combines columnar growth with a high plant density (Ruess, 2008; Jacob, 2004). The columnar growth of these trees originates from one dominant gene, which was discovered through a random mutation in the apple variety 'McIntosh' in 1960. Although the initial costs of planting a columnar apple orchard are relatively high due to the higher tree density, there are a lot of advantages of this orchard system compared to the regular spindle apple tree system (SATS). The columnar apple trees do not need a supporting stake, as stronger rootstocks are used. Since the tree shape is less wide and cylindrical, columnar trees can be planted at higher densities, offer better mechanization prospects and intercept light more homogenously. All of these advantages contribute to the expectation of higher yields per unit area of the CATS compared to the slender spindle planting system. Jacob (2004) even states that column apple varieties will allow a yield leap up to 150 tons of fresh weight per hectare, whereas SATS now yield about 60 tons of fresh weight per ha (Tromp *et al.*, 2005). However, it is not quite clear yet if this potential yield estimate of 150 tons of fresh weight per hectare is realistic and can be realized year after year without the occurrence of biennial bearing. Furthermore, it is not known yet if the dry matter content varies between the different apple varieties which are used in the two apple tree systems.

In practice apple tree spacing is related to mechanisation, since the arrangement of the trees should enable human and machine access for harvesting and cultural practices (Wagenmakers, 1991; Wagenmakers, 1995a, Tromp *et al.*, 2005). Furthermore, measures to control tree growth (e.g. fruiting and pruning) are affected by tree spacing, as these

measures should be adapted to the orchard system (Tromp *et al.*, 2005). Tree spacing additionally influences Leaf Area Index (LAI) and consequently the interception of photosynthetically active radiation (PAR: 400-700nm) per unit area (Wagenmakers and Callesen, 1995; Wagenmakers, 1991), which is the focus of this study.

According to Wagenmakers (1991) light interception can be manipulated by tree density and the arrangement of the trees at a certain density (spacing). Furthermore, tree shape and size are essential in light interception and distribution in orchard systems (Wagenmakers, 1991). Apple plantings with high tree densities intercept more light per unit area since the leaf area index is larger. This results in more canopy photosynthesis per unit area and accordingly larger fruit yields of orchards (Balkhoven-Baart *et al.*, 2000; Wagenmakers, 1995a and b; Wagenmakers and Callesen, 1995). However, the increase in light interception is accompanied by a higher level of shade in the canopy which might reduce the quality of the yield. Therefore, light interception should be optimized rather than maximized. Similar trees at a certain density arranged in a square design were found to enhance light interception as well as light distribution (Wagenmakers and Callesen, 1995; Wagenmakers, 1991; Tromp *et al.*, 2005). Adjusting tree height to alley width in determining tree density is important to take into account considering internal orchard canopy shading, which might result in yield of poor quality and top-dominant trees which are hard to maintain (Tromp *et al.,* 2005*)*, and cause loss of quality (couloration). The relationship between the level of apple production and light interception was found to be linear up to values of 80-90% of the available light. However, at these light interception values, apple quality aspects such as size and colour were found to be reduced (Wagenmakers and Callesen, 1995). Optimally, 70% of the available light should be intercepted in order to avoid enlarged internal shading, independent of the planting system, since the production of quality fruit was found to be maximal at this point (Tromp *et al.*, 2005; Wagenmakers and Callesen, 1995; Wagenmakers and Tazelaar, 1999). Hence, in this study the optimal plant spacing and density is defined as the plant spacing at which 70% of the available amount of PAR is intercepted by the canopy. Besides optimal light interception, adequate allocation of assimilates to the fruits is required aiming at a high yield of quality fruits (Tromp *et al.*, 1996; Wagenmakers and Callesen, 1995; Wagenmakers, 1991). *This study aims to obtain the optimal tree density and spacing of the columnar- (CATS) versus spindle apple tree system (SATS) by measuring and modelling their light interception and fruit production efficiency (dry weight yield per unit of PAR intercepted).*

2. METHODOLOGY

In order to fulfil the aim of this study, different destructive and non-destructive measurements were conducted for the SATS as well as the CATS. In this chapter the methodology on each non-destructive (Paragraph 2.2.1) and destructive (Paragraph 2.2.2) measurement will be explained, after the orchard characteristics were discussed in Paragraph 2.1.

2.1 Orchard characteristics

The two year old SATS (Elstar/M9) was located in Randwijk, The Netherlands (longitude 5.71°, latitude 51.94 °) and the direction of the orchard rows was north-south. The path width between the rows was 3.25m and the distance between the spindle trees in the rows was 0.80m. The two year old orchard rows of the CATS (Suncats/ MM111) were also directed north-south, whereas they were located in Wognum, The Netherlands (longitude 5.03 °, latitude 52.68 °). The columnar trees were planted 0.30m apart in the row, whereas the path width was 2.5m.

2.2 Measurements

In this chapter the methodology of each measurement was discussed, divided in non-destructive (PAR interception, tree height and tree width) and destructive measurements (leaf area, leaf weight, apple weight, apple diameter, apple blush colour).

2.2.1 Non-destructive measurements

2.2.1.1 PAR interception

Equipment
The SunScan Canopy Analysis system type SS1 from Delta-T Devices Ltd was used to measure PAR interception. The system consists of;

- SunScan Probe

The SunScan Probe is depicted in Figure 2.1. It consists of a light sensitive side of 1 m long containing 64 equally spaced photodiods measuring PAR (μmol m^{-2} s^{-1}). The total length of the probe is 1.04 m, of which the first 4 cm closest to the handle does not contain photodiods in order to avoid shadow of the handle of the probe. Via the probe handle the output of the photodiodes is converted into digital PAR readings, which are saved by the Psion Workabout through a cable. The probe has a wireless connection to the Beam Fraction Sensor (reference sensor of the light above the canopy) via an antenna. (Potter *et al.*, 1996)

Figure 2.1. SunScan Probe. (Source: Potter *et al.*, 1996)

- Beam Fraction Sensor

The Beam Fraction Sensor (depicted in Figure 2.2) monitors the amount of PAR incident on the canopy, which was used as the reference of the measurements beneath and within the canopy with the SunScan Probe. The difference between the two measurements refers to the amount of PAR intercepted by the canopy (μmol m^{-2} s^{-1}). Accordingly, the Beam Fraction Sensor should be located at a place within the orchard which is not shaded by any means.
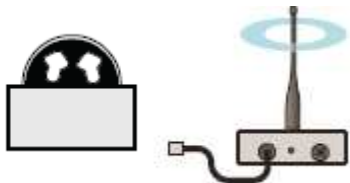

Figure 2.2. Beam Fraction Sensor (Source: Potter *et al.*, 1996)

- Data Collection Terminal (Psion Workabout)

The Psion Workabout is a device which is connected via a wire to the SunScan Probe and observes and stores the data from the probe. During the measurements it is possible to add notes to the data. Via the Psion Workabout the data can be transferred to an excel file on the computer, which allows for modification and further data-analysis. (Potter *et al.*, 1996)

Practical implications
The PAR interception measurements were performed within repeating units in the orchard, in order to justify extrapolation of the results to a larger surface area (ha^{-1}) and obtain a representative averaged estimation. The plot size was experimentally determined (Appendix I) as the distance between two trees until the middle of the path of both sides of

the trees, as depicted in Figure 2.3.
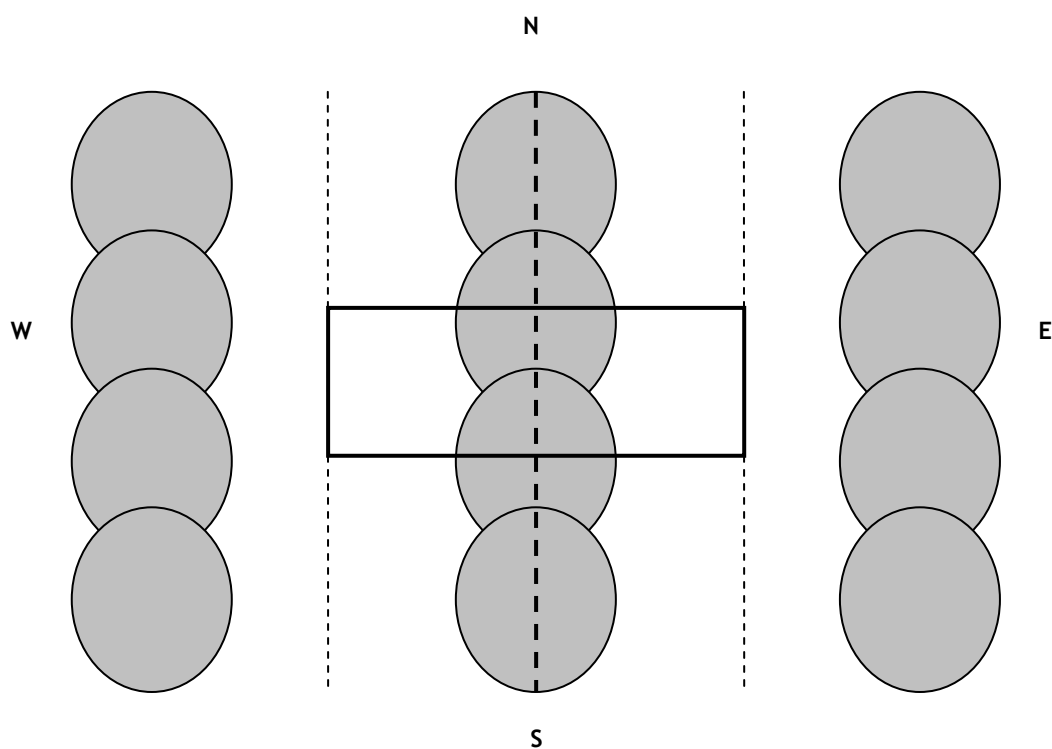
Figure 2.3. Size of one plot within the spindle apple tree system. The grey circles represent the spindle trees, whereas the th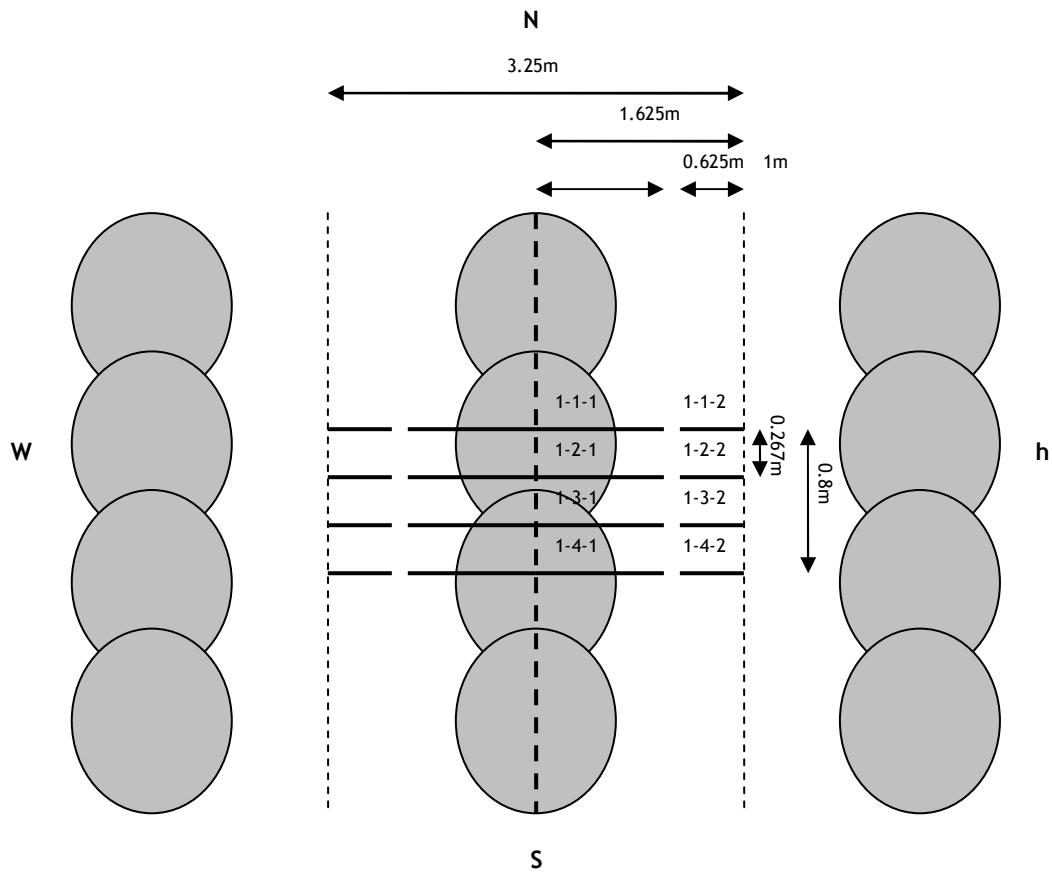ick dashed line shows the middle of the row and the thin dashed line the middle of the path. The distance between two trees in a row until the middle of the path on both sides of the trees represents one plot, which is depicted as a thick lined square.

Measurements were conducted approximately once every month (depending on the weather conditions) from flowering until harvest (Table 2.1). During dry weather conditions and preferably under a homogeneous diffuse sky the PAR interception measurements were conducted three hours before and after solar noon (10.00h, 13.00h and 16.00h). If it was not possible to measure under a homogeneous diffuse sky, measurements were conducted during homogeneous direct light conditions for both apple tree systems. Under direct light conditions, measurements were performed more often during the day (10.00h, 11.30h, 13.00h, 14.30h and 16.00h) since the effect of time of the day has a larger influence during these light conditions (Wünsche *et al.*, 1995).

Table 2.1. Measurement dates of the spindle- (SATS) and columnar apple tree system (CATS) in the year 2009.

SATS	CATS
7 May	8 May
28 May	4 June
1 July	23 June
4 August	6 August
10 September	9 September
16 September	23 September

Since half of the alley width of both the spindle and the columnar trees (1.625m and 1.25m respectively) is larger than the length of the SunScan Probe (1m), it was necessary to cover a part of the sensor in order to be able to measure half of the alley width (Figure 2.4 and 6). The effect of covering the sensor was tested (Appendix II) and resulted in a linear relation between the active length of the SunScan Probe and the percentage of PAR which was intercepted by the probe (Figure II.1, Appendix II).

Figure 2.4. Spatial arrangement of the PAR measurements of one plot within the spindle apple tree system. The grey circles represent the spindle trees, whereas the thick dashed line shows the middle of the row and the thin dashed line the middle of the path. The in total eight measurements were divided in two parts. Four PAR measurements were conducted with the total length of the SunScan Probe (1m) perpendicular to the row (1-1-1, 1-2-1, 1-3-1, 1-4-1). The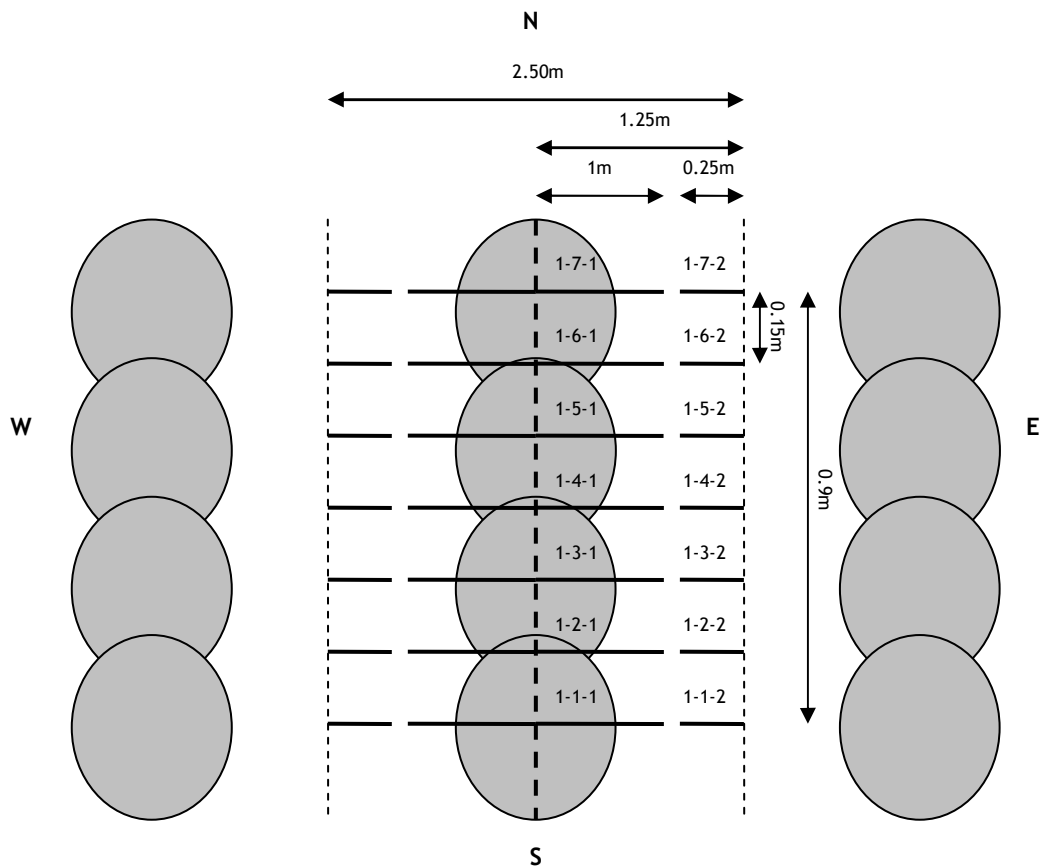 other four measurements (1-1-2, 1-2-2, 1-3-2, 1-4-2) were done while 0.375m of the SunScan probe was covered in order to be able to measure in total half of the path width (1.625m). This was done for three plots in total (each covering the east- and the west side of the row). The Beam Fraction Sensor was placed outside the row at a location which was not shaded by any means.

These PAR measurements in the SATS were repeated for in total three plots as is depicted in Figure 2.5. The plot location was chosen to be not too close to the hedge to avoid an influence of the shade of the hedge on the PAR interception measurements. Furthermore, by visual observation representative trees were chosen to be included in the plot (e.g. no large open spaces in the canopy in comparison to the other trees in the row) which were not close to an irregularity in the row or the neighbour rows (e.g. dead tree).
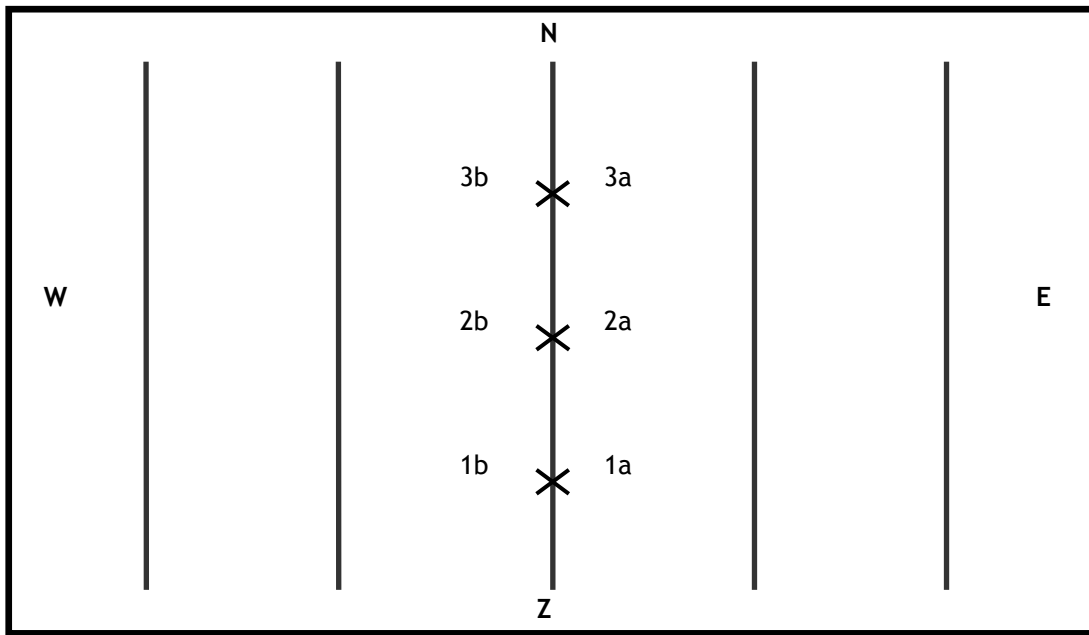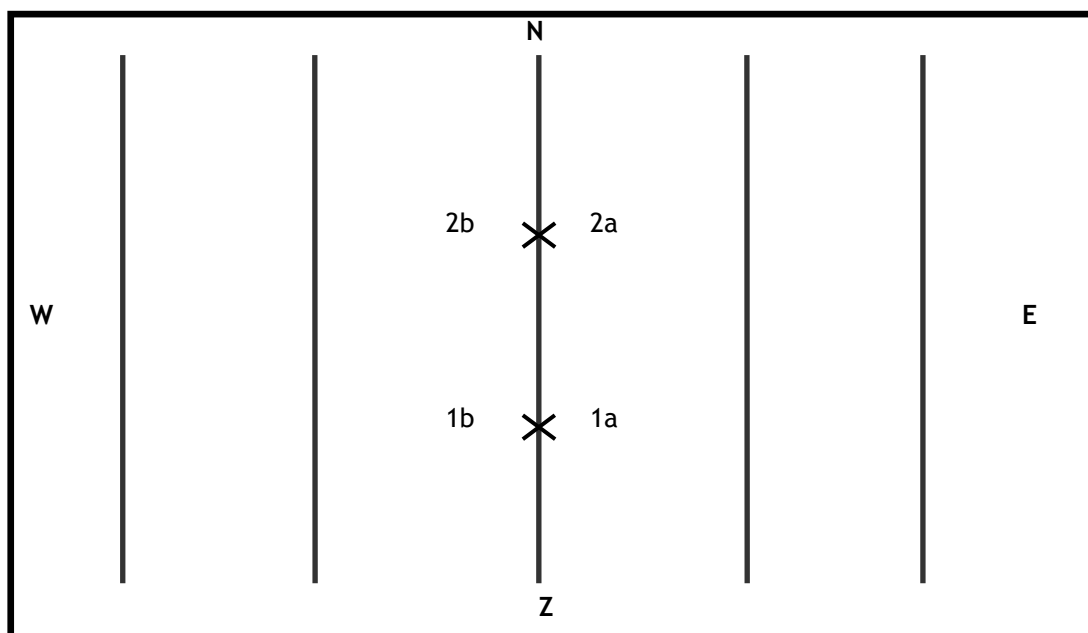
Figure 2.5. Spatial arrangement of the plots in the orchard row. The thick lined square represents the hedge of the orchard, whereas the thinner vertical lines depict the orchard rows. This picture is simplified; in reality there were more orchard rows surrounding the row in which the plots were located. The length of the row was 50m and the width of the field was approximately 325m. The crosses in the middle row show the location of one plot were b corresponds to the west side and a to the east side of the plot.

Figure 6 represents the spatial arrangement of the PAR interception measurements in the CATS. Since the distance between the trees in the row is much smaller in this orchard system compared to the SATS, the length of the plot (north-south direction) was adapted which also increased the amount of PAR measurements. Otherwise the PAR interception measurements would have to be taken too close to each other. Furthermore, incorporating more trees in the plot gives a more representative view of the whole orchard. Another criterion was that the larger number of measurements per plot did not exceed the time available for one PAR interception measurement at a certain time of the day (1h). Figure 2.6 depicts the arrangement of measurements in one plot for the CATS.

Figure 2.6. Spatial arrangement of the PAR measurements within one plot of the columnar tree apple orchard system. The grey circles represent the columnar trees, whereas the thick dashed line shows the middle of the row and the thin dashed line the middle of the path. The in total fourteen measurements were divided in two parts. Seven PAR measurements were conducted with the total length of the SunScan Probe (1m) of the row perpendicular to the row (1-1-1, 1-2-1, 1-3-1, 1-4-1, 1-5-1, 1-6-1, 1-7-1). The other seven measurements (1-1-2, 1-2-2, 1-3-2, 1-4-2, 1-5-2, 1-6-2, 1-7-2) were done while 0.75m of the SunScan probe was covered in order to be able to measure in total half of the path width (1.25m). This was done for two plots both covering the east side- and the west side of the row. The Beam Fraction Sensor was placed outside the row at a location which was not shaded by any means.

In the columnar apple tree system these PAR measurements were only repeated for in total two plots, as is depicted in Figure 2.7. Since there were not that much columnar trees of the same variety available, a third plot was not feasible.

Figure 2.7. Spatial arrangement of the plots in the orchard row. The thick lined square represents the hedge of the orchard, whereas the thinner vertical lines depict the orchard rows. This picture is simplified; in reality there were more orchard rows surrounding the row which in which the plots were located. However only the row on the right hand side of the row which was used for the measurements consisted of columnar apple tree. The other rows consisted of columnar shaped pear trees. The length of the rows was 50m and the average width of the field was 24m. The crosses in the middle row show the location of a combination of plots (e.g. 1a and 1b).

First PAR interception of each plot on the east side of the row were measured; 1a, 2a and 3a (the latter only in the SATS). Afterwards the plots on the west side of the row (1b, 2b - and 3b only in the SATS) were measured, so the time lap between a measurement of a plot on the east side of the row and the corresponding plot on the west side of the row (e.g. 1a and 1b) was approximately the same for each combination of plots.

The PAR interception measurements were conducted below the canopy and at two heights within the canopy (Figure 2.8). The PAR interception measurements below the canopy explain the PAR interception of the whole canopy, while the measurements at the other heights only show the PAR interception of a part of the canopy. This was done in order to be able to see the influence of canopy shape (cone versus cylinder) on PAR interception. The different heights were determined by dividing the volume of the tree canopy by three, since it was assumed that per tree volume the same leaf area is present. For the columnar trees this was done simply by dividing the canopy height by three, since the canopy was assumed to have a cylindrical shape. The spindle trees however have more or less a cone shaped canopy which requires a more complicated calculation of the measurement heights (Appendix IV).
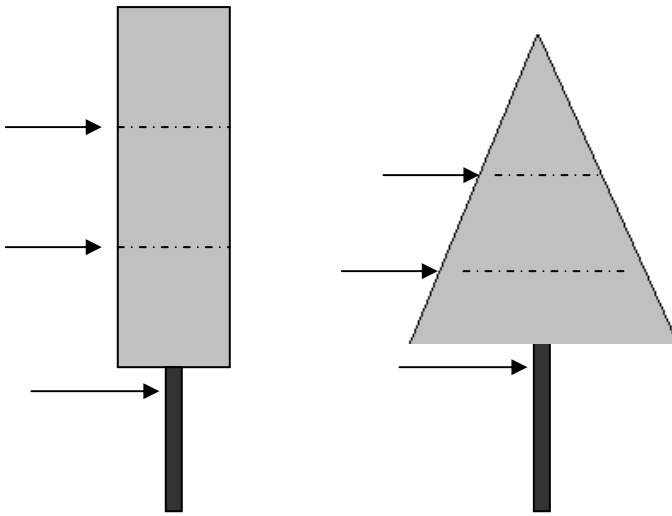
Figure 2.8. Height positions of the PAR measurements. The picture on the left depicts a columnar apple tree and the picture on the right depicts a spindle apple tree. The arrows indicate the approximate height of the PAR interception measurements, which was determined by dividing the canopy volume by three.

Occasionally a measurement above the canopy with the 'light sensitive part' of the SunScan Probe directed to the canopy was done in order to estimate reflection of the canopy. Also reflection of the soil was measured using the same method near the soil surface.

Analysis

In order to determine the fraction PAR intercepted measured at the different heights in one plot for the spindle- and columnar apple tree system, Equation 1 and Equation 2 were used respectively.

$$F_i = \frac{\sum_{i=1}^{4}[I_{0i}-I_i]+\sum_{i=5}^{8}[0.625 \cdot I_{0i}-I_i]}{\sum_{i=1}^{4}I_{0i}+\sum_{i=5}^{8}0.625 \cdot I_{0i}} \qquad \textit{Equation 1}$$

$$F_i = \frac{\sum_{i=1}^{7}[I_{0i}-I_i]+\sum_{i=8}^{14}[0.25 \cdot I_{0i}-I_i]}{\sum_{i=1}^{7}I_{0i}+\sum_{i=8}^{14}0.25 \cdot I_{0i}} \qquad \textit{Equation 2}$$

The first term of the numerator in both equations represents the sum of PAR interception (global PAR (I_{0i}) - PAR intercepted by the SunScan Probe at a certain height in the tree (I_i)) of the part of the plot which was measured with the total active length of the SunScan Probe (1m). This was added to the sum of the PAR interception measurements done with the partly covered SunScan Probe (0.625m for the SATS and 0.25m for the CATS). The entire numerator was subsequently divided by the sum of the global PAR measured during the first measurements (four for the SATS and seven for the CATS, using 1m active SunScan Probe

length) plus the global PAR measured during the second measurements (using the partly covered SunScan Probe). Appendix IV explains the exact derivation of these equations.

2.2.1.2 Tree height and canopy diameter

Before each PAR interception measurement the average height and width (canopy diameter) of the trees in the plots were determined. The length of the stem (starting at the soil surface) and the length of the canopy (starting at the first branch) were measured separately in order to be able to determine the different heights in the tree canopy where the PAR interception measurements should take place. The canopy diameter was also determined in order to be able to calculate the measurement heights for PAR interception (as was explained in Figure 2.8). The average of line a and b in Figure 2.9 measured below the canopy for all trees in a plot was used as the value for canopy diameter.
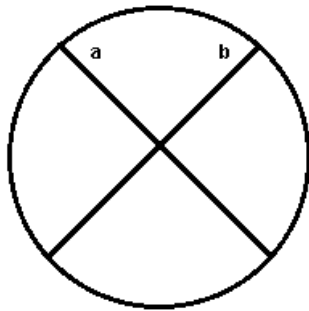
Figure 2.9. Determination of tree diameter. The circle represents one tree in a plot. For all trees in a plot the average length of line a and b, measured directly below the canopy, was determined. The average of these values for all trees in a plot was finally used as canopy diameter.

2.2.2 Destructive measurements

In this chapter the methodology on the destructive measurements on the leaves (leaf area, leaf weight) and the apples (apple diameter, apple weight, apple blush colour) of the SATS and the CATS were explained.

2.2.2.1 Leaves

Leaf Area Index (LAI)

All leaves of a plot were counted on the same day as the PAR interception measurement was conducted. The plot used was not exactly the same as was used for the PAR interception measurements (picking the leaves of this plot would influence the PAR interception measurement) but it was located in the same orchard row and had the same size (2.60 and 2.25m^2 for the SATS and the CATS, respectively). A sample of 10% of the total number of leaves was picked and the leaf area of these leaves was measured using a leaf area meter (LI-3100 Area Meter) and multiplied by the total number of leaves in the plot (Wünsche and Palmer, 1998). Accordingly the LAI (m^2 m^{-2}) was calculated by dividing the leaf area of the whole plot by the total surface area occupied by the plot (3.25m·0.80m=2.60m^2 and 2.50m·0.90m=2.25m^2 for the SATS and CATS respectively).

Specific Leaf Area

The same leaves as were used for determining the LAI were used in order to determine the dry weight of the leaves in the plot. After the leaves were used for the LAI determination, fresh weight was determined by weighing on a Mettler PE 500 scale (in grams with an accuracy of two decimals). The leaves were again weighted on this scale after drying them for 24 hours at a temperature of 105°C in a ventilated oven (Memmert UM 500). Hence, the SLA (m^2 g^{-1}) could be calculated by dividing the total leaf area by the total dry weight of the leaves.

2.2.2.2 Apples

Apple diameter

The diameter of the apples were determined after each PAR interception measurement of the same plot as was used for the LAI and SLA measurements (Chapter 2.2.2.1). The number of apples in the plot were counted, where after a sample of 10% of the apples were picked and weighted. Half of the number of apples of the sample were picked at the west- and half at the east side of the row at different heights in the tree canopy. The diameter of the apples was determined with the digital callipers Mitutoyo 500. The diameter was expressed in mm with an accuracy of two decimals. The average of two measurements per fruit perpendicular to each other was used as the apple diameter.

Apple weight

The same sample as was used for determining the apple diameter was afterwards used for measuring the apple weight. The fresh weight of each apple was determined by weighing on a Mettler PE 500 scale (in grams with an accuracy of two decimals). The dry weight was determined in the same way and with the same accuracy, after the fruits were sliced in smaller pieces and dried for minimally 24 hours at a temperature of 105°C in a ventilated oven (Memmert UM 500). From the fresh- and dry weight respectively of the apples in the sample, the fresh- and dry weight of the total plot was calculated. Subsequently, the fresh- and dry weight of the apples in the plot were multiplied by the number of plots which fit in 1 ha, in order to determine the fresh- and dry weight yield per ha. Also the fraction dry weight was calculated by dividing the dry weight of the apple yield (g ha^{-1}) by the fresh weight apple yield (g ha^{-1}).

Apple colouration

The total harvest of one plot of both apple tree systems was used for measuring the blush area (% blush on total apple surface) of the apples with the AWETA colour camera in combination with the AWENORM programme. While the apples were rotated under the camera (one at the time) via a small assembly line, pictures were taken. In this way the full surface of the apple was scanned. The percentage red colour (blush) using Elstar settings as

a reference, was accordingly measured. The blush area was displayed on a connected computer via the programme AWENORM.

2.3 Theory light interception in row crop canopies

In this chapter the theoretical background of PAR interception in row crop canopies is explained according to Goudriaan (1977).

2.3.1 Homogeneous crop canopies

Homogeneous crop canopies have by definition an evenly distributed leaf area over the entire soil surface which is occupied by the crop. The fraction of radiation intercepted (F_i) by a homogeneous canopy (ignoring reflection by the canopy) can be explained by an exponential extinction function of the leaf area index (*LAI*):

$$I = I_0 \cdot e^{-k \cdot LAI}$$

Equation 1

Where

I   *= radiation intensity below the plant canopy*
I_0 *= radiation intensity above the plant canopy*
k   *= radiation extinction coefficient*
LAI   *= leaf area index = leaf area/ surface area*

Accordingly, the fraction of radiation intercepted by a homogeneous canopy can be described as the amount of radiation intercepted by the canopy (the difference between the radiation intensity above and below the canopy) divided by the radiation intensity above the canopy:

$$F_i = \frac{I_0 - I}{I_0}$$

Equation 2

If *I* in equation 2 is substituted by $I_0 \cdot e^{-k \cdot LAI}$ according to equation 1, this results via calculation step 2c in equation 3.

$$F_i = \frac{I_0 - \left(I_0 \cdot e^{-k \cdot LAI}\right)}{I_0}$$

Equation 2b

$$F_i = \frac{I_0 \cdot \left(1 - e^{-k \cdot LAI}\right)}{I_0}$$

Equation 2c

$$F_i = 1 - e^{-k \cdot LAI}$$

Equation 3

2.3.2 Row crop canopies

2.3.2.1 Compressed canopy
Alternating bare paths and rows including the crop define row crops (Figure 2.10).

Incoming radiation

Row   Path   Row
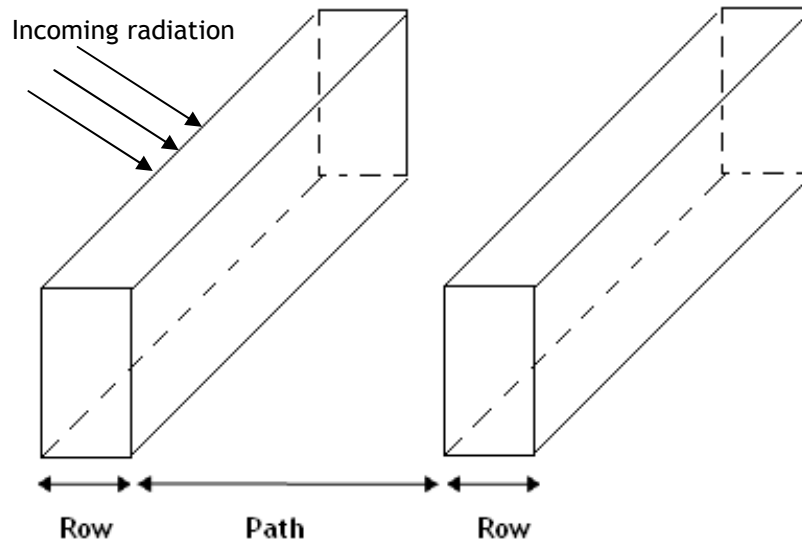
Figure 2.10 Schematic illustration of radiation interception of a row crop. (Source: Modified from Pronk *et al.*, 2003)

The leaves of the row crop are concentrated in the rows whereas they are absent in the paths. However, the leaf areas remain the same as compared to homogeneous crops. In row crops the leaf area can be considered to be 'compressed' in the row versus zero in the bare path. If all rows would be pushed together, the compressed leaf area index (LAI_{comp}) would be:

$$LAI_{comp} = LAI \cdot \frac{R+P}{R}$$
Equation 4

Where

R   = *row width (width between the plants in the row)*
P   = *path width*

Equation 4 can be explained as follows:

$$LAI = \frac{LA}{R+P}$$

and

$$LAI_{comp} = \frac{LA}{R}$$

Consequently the factor ($\frac{R+P}{R}$) is needed to convert *LAI* in *LAI*$_{comp}$ as is described in equation 4.

In line with equation 1 the radiation level below the compressed canopy becomes:

$$I_{comp} = I_0 \cdot e^{-k \cdot LAI_{comp}}$$

Equation 5

Now the fraction of radiation intercepted by the compressed canopy can be calculated (6). Besides the necessary conversion of *LAI* in *LAI_{comp}*, equation 6 accounts for the fraction of soil area covered by the crop ($\frac{R}{R+P}$):

$$F_{i,comp} = \frac{R}{R+P} \cdot \left(1 - e^{-k \cdot LAI_{comp}}\right)$$

Equation 6

2.3.2.2 Black canopy with infinite LAI

In the theoretical case of a black plant row with a infinite leaf area index, radiation cannot penetrate through the canopy. Consequently only radiation passing through the space of the path can reach the soil surface. This fraction of radiation reaching the soil surface for a specific point at the soil surface can be calculated if path width (p), row width (r) and row height (h) are known. In Pronk *et al.* (2003) this is called the view factor of the sky onto the path(Figure 2.11).
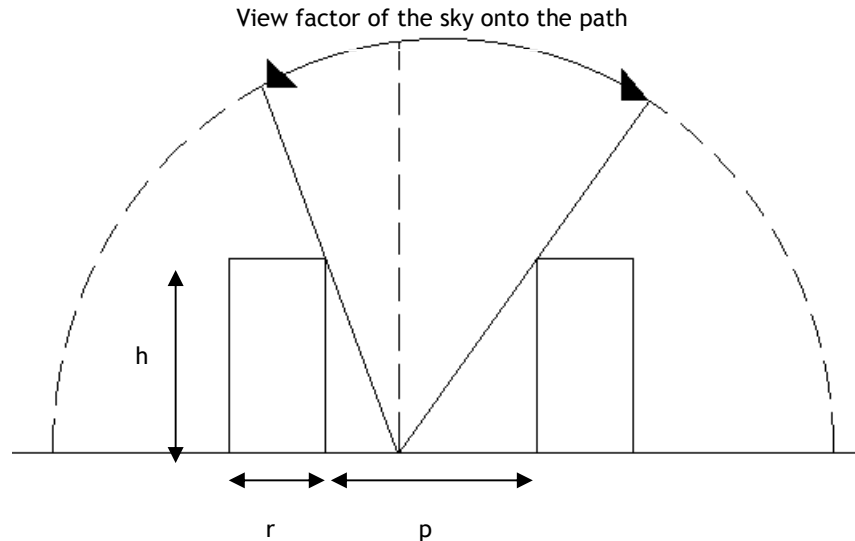
Figure 2.11 Viewfactor of the sky onto the path (after Pronk *et al.*, 2003), assuming a black non-infinite leaf area index. h=plant height, r=row width and p=path width.

Spatially integrated over the path according to Appendix V, the relative radiation onto the path (I_p) becomes:

$$I_p = \frac{\sqrt{h^2+p^2}-h}{p}$$

Equation 7

However, in the realistic situation of a non-infinite LAI, a certain level of radiation will penetrate through the canopy which increases I_p. Gijzen and Goudriaan (1989) developed a method which allows estimation of the number of rows through which radiation passes, however in this thesis a simplified method will be used according to Pronk *et al.*(2003).
In order to calculate the radiation level at the soil in the path in the situation of a non-infinite LAI (S_p); the factor which accounts for the extinction of radiation penetrating through the canopy (e^{-k*LAI}) multiplied by the complement of I_p, was added to I_p:

$$S_p = I_p + (1 - I_p) \cdot e^{-k \cdot LAI}$$

Equation 8

In order to calculate the radiation level at the soil in the row (underneath the canopy)(S_r) a similar approach can be used. First the view factor of the sky onto the row (Figure 2.12) was used to determine the radiation level at one point at the soil in the row assuming an infinite LAI.
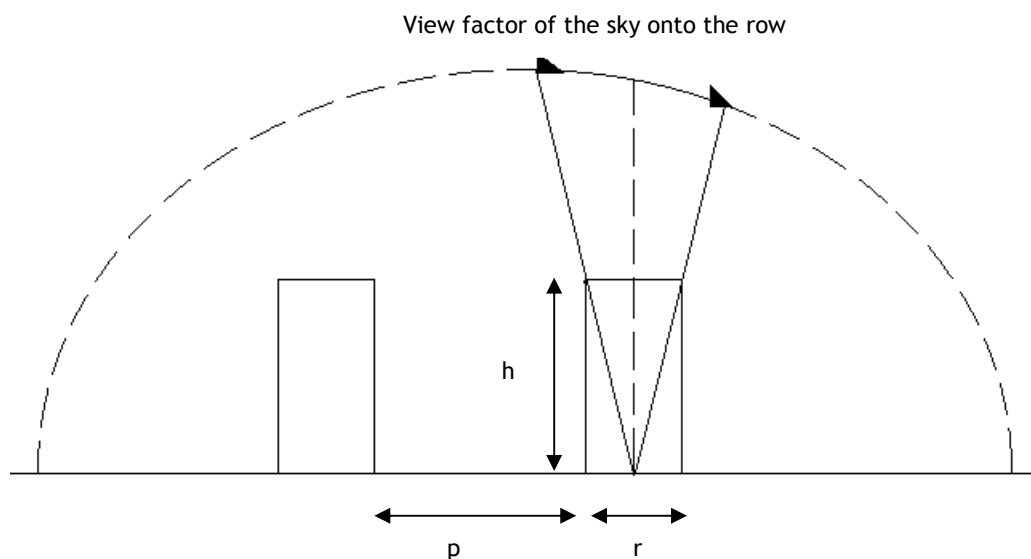
Figure 2.12 View factor of the sky onto the row (after Pronk *et al.*, 2003), assuming a black non-infinite leaf area index. h=plant height, r=row width and p=path width.

Spatially integrated over the row (similar to Equation 7, see Appendix V), the relative irradiance onto the row of a black row crop with an infinite LAI (I_r) became:

$$I_r = \frac{\sqrt{(h^2+r^2)}-h}{r}$$

Equation 9

Using I_r, the radiation level at the soil in the row (underneath the canopy) assuming a non-infinite LAI (S_r) can be calculated similar to Equation 8. However, to avoid overestimation of I_r, the extinction of the radiation penetrating through the row itself should be taken into account ($e^{-k*LAIcomp} = I_{comp}/I_0$):

$$S_r = I_r \cdot \frac{I_{comp}}{I_0} + (1 - I_r) \cdot e^{-k \cdot LAI}$$

Equation 10

2.3.3 Fraction radiation intercepted

Depending on the path width (p), row width (r) and canopy height (h), the heterogeneity of a row crop with a given LAI differs. There is no difference between a row crop canopy and a homogeneous canopy if the row- and path widths are much smaller than the canopy height. Using Equation 1 will do in this case. However in the opposite case of relative large row- and path widths, the compressed LAI approach (as explained above) is more realistic. Accordingly, the degree of heterogeneity can be explained by the relative difference between the radiation at the soil surface beneath the plant row and the path $(S_p-S_r)/(I-I_{comp}/I_0)$.

Hence, The total fraction of radiation intercepted by a row crop canopy can be explained by the approximating equation:

$$F_{i,rowcrop} = F_i - \frac{(F_i - F_{i,comp}) \cdot (S_p - S_r)}{\left(I - \frac{I_{comp}}{I_0}\right)}$$

Equation 11

In a homogeneous canopy or in a row crop canopy where the row- and path widths are much smaller than the canopy height, S_p and S_r will be approximately identical, so the whole term after F_i becomes zero. If the path width is relatively large compared to the canopy height, the factor $(S_p-S_r)/(1-(I_{comp}/I_0))$ becomes larger, indicating more heterogeneity. If the latter factor is 1 (since it is a relative factor, the value will be between 0 and 1), $F_{i, row crop}=F_i-(F_i-F_{i, comp})*1=F_{i,comp}$.

2.3.4 Model

In the programme ROWCROP developed by Goudriaan (1977), this theoretical background on PAR interception in row crop canopies was implemented. The leaf area index (LAI), extinction coefficient (k), plant height (h), row width (r) and path width (p), were used as inputs in this model in order to obtain the fraction PAR intercepted by the row crop as output. Except for the extinction coefficient, all inputs were directly obtained from the measurements. Via trial and error was determined which extinction coefficient (k) was used as model input in order to gain a fraction PAR intercepted as model output which was closest to the total fraction PAR intercepted retrieved by the measurements (at the low measurement height). In Appendix VII the programme ROWCROP can be found.

2.3.4.1 Sensitivity analysis

Since there was a discrepancy between the fraction PAR intercepted measured and the fraction PAR intercepted calculated via ROWCROP (Chapter 3.1.3, Figure 8), a sensitivity analysis was conducted in order to determine the parameters that have the most effect on the model outcome (fraction PAR intercepted). As a measure for sensitivity, elasticity was used (Leffelaar and Scholten, 2010) to calculate the relative influence of a deviation of 10, 5, 2.5 and 1% around the default value of the experimentally determined model input parameters h (tree height), p (path width), w (width between the trees), k (extinction coefficient) and LAI on the model output $F_{i,rowcrop}$ (Equation A). Assuming that every parameter was independent.

$$E_{F_{i,rowcrop},\ p,\ t} = \frac{\left(\dfrac{F_{i,rowcrop,\ t,\ p=max}\ -\ F_{i,rowcrop,\ t,\ p=min}}{F_{i,rowcrop,\ t,\ p=default}}\right)}{\dfrac{p_{max}\ -\ p_{min}}{p_{default}}}$$

Equation A

With:

$E_{F_{i,rowcrop},\ t,\ p}$	:	elasticity of $F_{i,rowcrop}$ to parameter p at time=t;
$F_{i,rowcrop,\ t,\ p=max}$	:	$F_{i,rowcrop}$ at time=t and the maximum value of parameter p over its (changed) range;
$F_{i,rowcrop,\ t,\ p=min}$	:	$F_{i,rowcrop}$ at time=t and the minimum value of parameter p over its (changed) range;
$F_{i,rowcrop,\ t,\ p=default}$	:	$F_{i,rowcrop}$ at time=t and the default value of parameter p;
p_{max}	:	maximum value of parameter p over its (changed) range;
p_{min}	:	minimum value of parameter p over its (changed) range;
$p_{default}$	:	default value of parameter p

In Table III.1 and III.2 of Appendix III, the elasticity of $F_{i,rowcrop}$ to parameters h, p, w, k, and LAI at 10, 5, 2.5 and 1% deviation around the default value for the columnar- and spindle apple tree system are presented respectively. For both apple orchard systems no difference was found between the elasticity of $F_{i,rowcrop}$ for 10, 5, 2.5 and 1% deviation around the default value per parameter at a certain measurement date (Appendix VIII). Since a range of 10-1% is reasonable, most likely the values for elasticity are accurate. Hence the smallest deviation (1%) around the default value was used to determine the relative influence of the different parameters on $F_{i,rowcrop}$ (Figure 2.13).
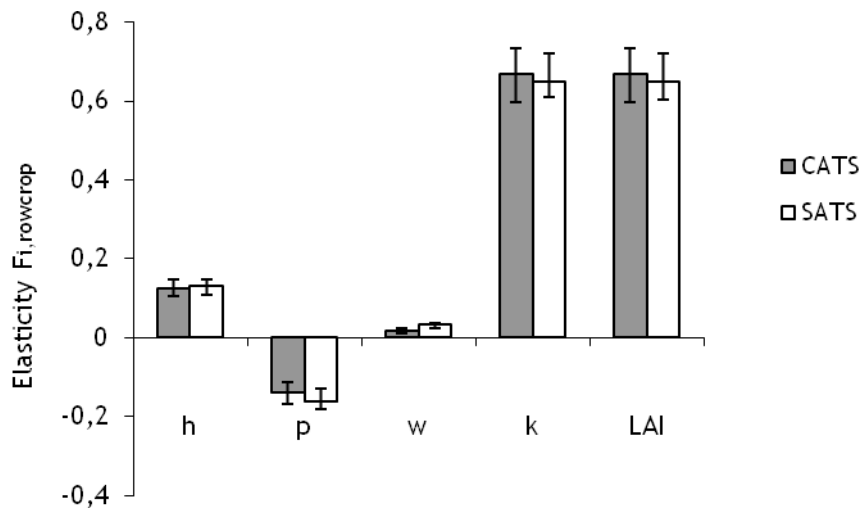
Figure 2.13. Average elasticity of $F_{i,rowcrop}$ over all six measurement dates to parameters h, p, w, k and LAI at a 1% deviation around the default value for the columnar- (CATS) and spindle apple tree system (SATS). The ranges represent the difference between the highest and lowest parameter value over the six measurement dates and the default value of the parameter.

The values for elasticity of $F_{i,rowcrop}$ to all parameters (Figure 2.13) were converted into terms of sensitivity of the model to the parameters, assuming that; $0 < E_{Fi,rowcrop, p, t} < 0.1$ is rather insensitive, $0.1 < E_{Fi,rowcrop, p, t} < 0.5$ is not very sensitive and $0.5 < E_{Fi,rowcrop, p, t} < 1$ is sensitive. Accordingly parameter w is rather insensitive, parameters h and p are not very sensitive and parameters k and LAI are sensitive. Only parameter p has a negative elasticity, since $F_{i,rowcrop}$ decreases at an increasing path width (p). The parameters k and LAI have the largest elasticity values and thus the largest influence on $F_{i,rowcrop}$. Since parameters k and LAI are both in the same power term in the equations used in ROWCROP (e^{-k*LAI}), they cancel each other out which results in approximately the same sensitivity of the model to k and LAI. If the model reacts sensitive to parameters (like k and LAI) it is very important that the values for these parameters are correct and therefore accurately determined. However, in this experiment the less sensitive parameters (p, h and w) could be measured most precise. In order to determine the LAI, the leaf area of a sample of approximately 10% of the total amount of leaves in the plot was measured. Inaccuracies could have been occurred since only 10% of the leaves were measured (not all leaves) and by counting the large amount of leaves per plot. Furthermore a lot of information is incorporated in parameter k (e.g. tree architecture). This parameter was determined via trial and error, which might not be the most accurate method. However it was not possible to derive k analytically from the equations used in ROWCROP.

3. RESULTS

The results of all measurements, separated in non-destructive- (Paragraph 3.1) and destructive measurements (Paragraph 3.2), are presented in this chapter. Paragraph 3.1 considers the results of the PAR interception measurements; the influence of different moments during a day, different plots and side of the row (east or west) on fraction PAR intercepted by the two apple tree systems (CATS and SATS). Whereas Paragraph 3.2 shows the results of the destructive measurements on the leaves (specific leaf area and leaf area index) and apples (weight, diameter and blush colour) over time. Furthermore, the results of the non-destructive PAR interception measurements and the destructive apple weight were combined in Paragraph 3.3 (Apple production efficiency) and applied in Paragraph 3.4 (Model PAR interception).

Since for each apple tree system only six measurements were done, the number of observations (n) were never larger than n=6. This small n is the reason why no variance was calculated within this research. In order to visualise the variability of the data in graphs, besides the mean values, the lowest and highest values of which this mean was composed were shown by the range.

3.1 Non-destructive measurements

3.1.1 PAR interception

For the spindle- (SATS) and the columnar apple tree system (CATS), the trend in fraction PAR intercepted (average over the plots and different measurement times during a day) from flowering till harvest seems similar for each measurement height (see Figure 3.1). The total fraction PAR intercepted by the tree (measured at the low measurement height) was highest, followed by the fraction PAR interception found at the middle and high measurement heights respectively.

Furthermore, for both apple tree systems the fraction PAR intercepted shows an overall increase over time (for the low, middle and high measurement heights respectively from 0.29 to 0.35, 0.21 to 0.23 and 0.13 to 0.16 for the SATS, and from 0.23 to 0.41, 0.16 to 0.31 and 0.07 to 0.08 for the CATS) which was largest for the low measurement height. Moreover, the overall increase in PAR interception was larger for the CATS at the low and middle measurement heights.

Despite the overall increase in fraction PAR intercepted by both apple tree systems, a decrease was shown from August onwards. However at the middle measurement height of the SATS, this decrease already started from the measurement conducted at the 1st of July onwards. For the CATS the decrease starts at the measurements conducted at the 6th of August, while the PAR interception seems to increase slightly again from just before to just after harvest (from 9 to 23 September).

Average over the whole period of measurements the total fraction PAR intercepted (low measurement height) was 0.37 for the SATS and 0.34 for the CATS.
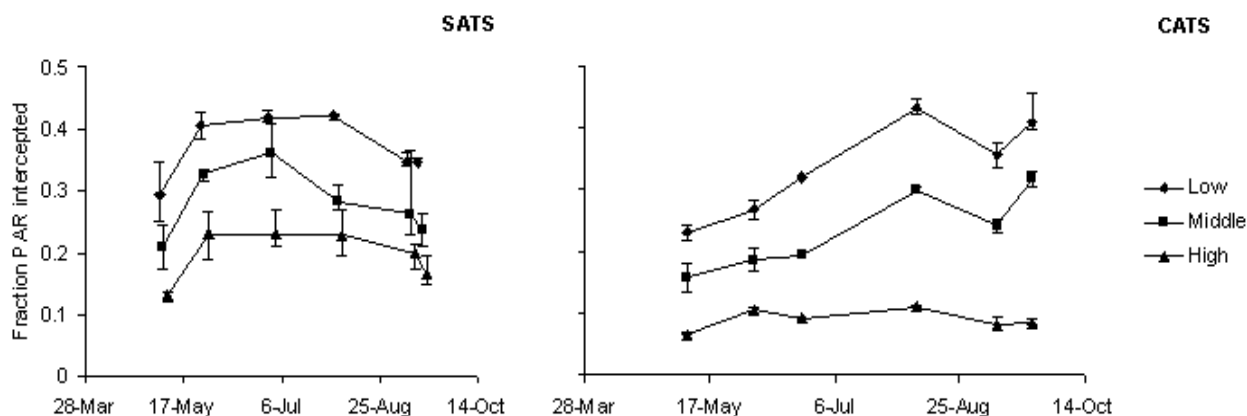
Figure 3.1. Fraction PAR intercepted by the spindle- (SATS) and columnar (CATS) apple tree systems (average over the different plots and measurement times during a day) from flowering till right after harvest, depicted per apple tree systems for the low, middle and high measurement heights. Measurements were done approximately once a month (from flowering till right after harvest) three times during a day during diffuse-, and five times during a day during direct light conditions. Except for the third and the fourth measurements, which were done during homogeneous direct light conditions, the measurements were conducted during homogeneous diffuse light conditions. All measurements of one apple tree system were done at the same day, however the measurement dates in the graph for the middle and high measurement height where adapted (shifted to two days before and after the actual measurement date, respectively) in order to avoid overlapping ranges. The ranges depict the highest and lowest fraction of PAR intercepted measured within the plots (three plots for the SATS, and two for the CATS), describing the variability in PAR interception between the different plots.

In Figure VI.1 of Appendix VI, the fraction PAR intercepted (average over the measurement times during a day) by both apple tree systems for each measurement height (low, middle and high) per plot can be found.

Figure 3.2 depicts the differences in PAR interception per measurement height, in order to be able to compare the differences in PAR interception (average over the different plots and measurement times during a day) between the SATS and the CATS. The CATS starts off intercepting a lower fraction of PAR than the SATS for all three measurement heights. However, during the first four measurements (from the beginning of May to the beginning of August) the CATS showed a faster increasing trend, which results in a slightly higher fraction PAR intercepted compared to SATS after harvest. Still, at the high measurement height the fraction PAR intercepted by the CATS was lower compared to the SATS, during the whole growing season.
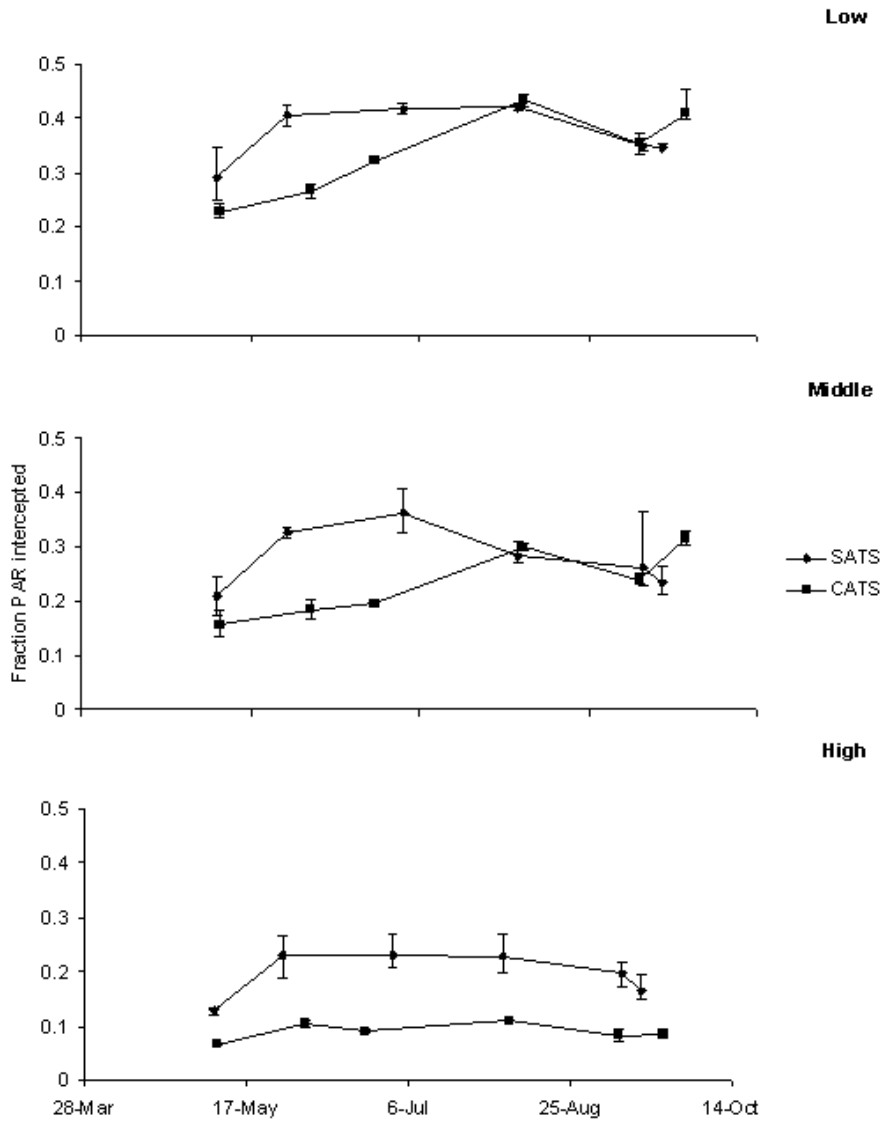
Figure 3.2. Fraction PAR intercepted by the spindle- (SATS) and columnar (CATS) apple tree systems (average over the different plots and measurement times during a day) from flowering till right after harvest, depicted per measurement height (low, middle and high) for both apple tree systems. Measurements were done approximately once a month (from flowering till right after harvest), three times during a day during diffuse-, and five times during a day during direct light conditions. Except for the third and the fourth measurements, which were done during homogeneous direct light conditions, the measurements were conducted during homogeneous diffuse light conditions. The ranges depict the highest and lowest fraction of PAR intercepted measured within the plots (three plots for the SATS, and two for the CATS), describing the variability in PAR interception between the different plots.

The effect of time of day on fraction PAR intercepted (average over the different plots) by both apple tree systems was presented in Figure 3.3. At each measurement height, differences in PAR interception between the measurement times during a day (10.00h, 13.00h and 16.00h for each measurement date, except for 1 July and 4 August for the SATS

and 23 June and 6 August for the CATS, where measurements were also conducted at 11.30h and 14.30h) were observed for both apple tree systems. These differences were similar for each measurement height, when PAR interception was measured at a certain date. In the CATS the fraction PAR intercepted at 10.00h seems almost always lowest, whereas the highest fraction PAR intercepted was most often found at 16.00h. However no such trend was shown by the SATS. During the measurements conducted under direct light conditions, the variability between the measurement times during a day seems larger for the CATS (23rd of June and 6th of August), while for the SATS this seems to be only the case for one of the measurements conducted during direct light conditions (4th of August).
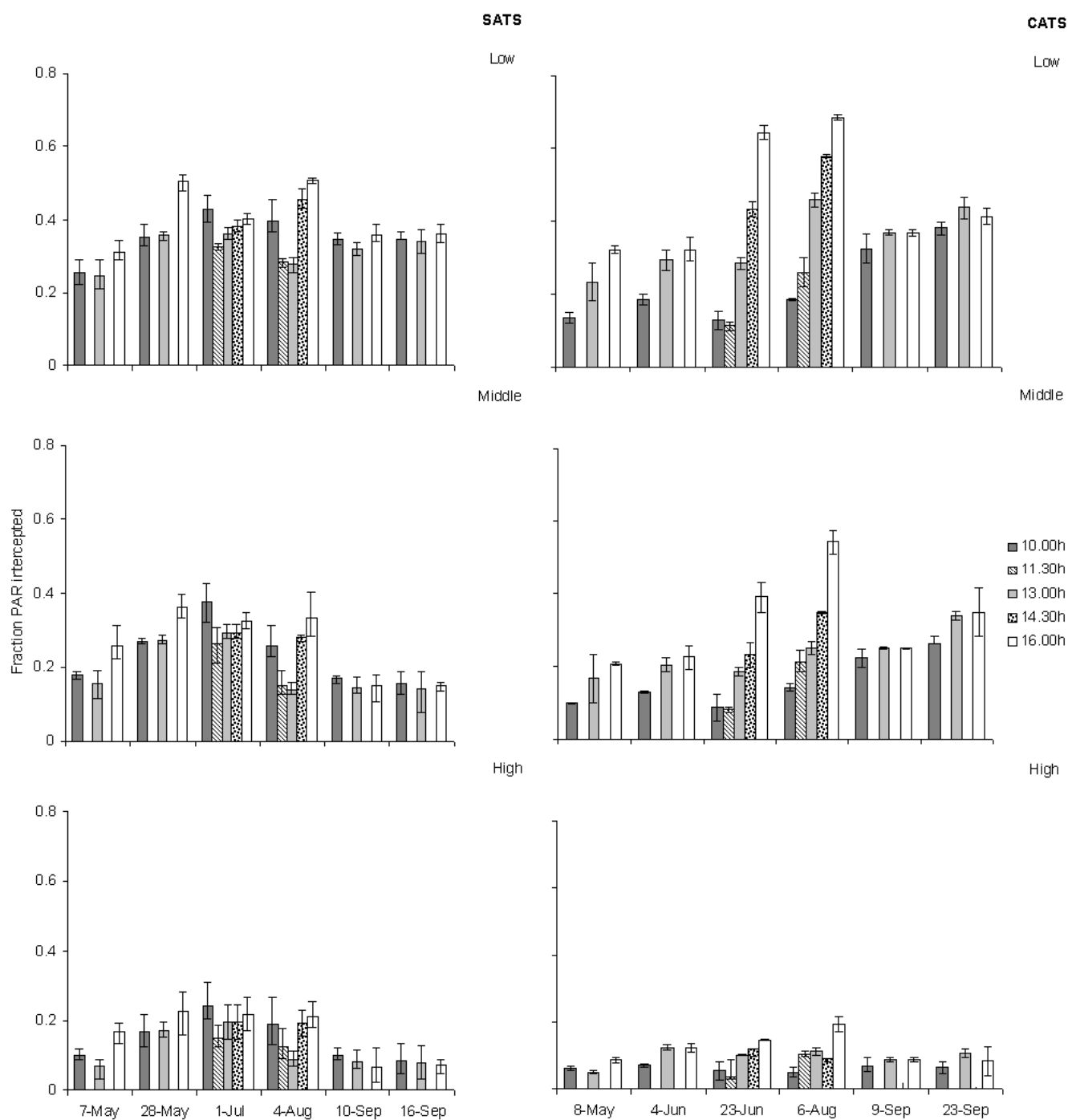
Figure 3.3. Fraction PAR intercepted by the spindle- (SATS) and columnar (CATS) apple tree system (average over the different plots) from flowering till right after harvest, depicted per measurement height (low, middle and high) for the different measurement times during a day (10.00h, 11.30h, 13.00h, 14.30h and 16.00h). Measurements were done approximately once a month (from flowering till right after harvest), three times during a day during diffuse- (10.00h, 13.00h and 16.00h) and five times during a day (10.00h, 11.30h, 13.00h, 14.30h and 16.00h) during direct light conditions. Except for the third and the fourth measurement, which were done during homogeneous direct light conditions, the measurements were conducted during homogeneous diffuse light conditions. The ranges depict the highest and lowest fraction of PAR intercepted measured within the different plots

(three plots for the SATS, and two for the CATS), describing the variability in PAR interception between the different plots.

Figure 3.4 shows the influence of the side of the row (east or west) on the fraction PAR intercepted by the trees (average over the plots, measured at solar noon in order to neglect the influence of time of day). Both apple tree systems show a difference in PAR interception between the east and west side of the row. This difference seems largest for the measurements conducted during direct light conditions for the CATS (June 23rd and August 6th). The east side of the row intercepts the largest fraction of PAR during all measurements at each measurement height for the SATS. For the CATS, this is not the case for each measurement height for the measurements done at the 4th of June and the 23rd of September.
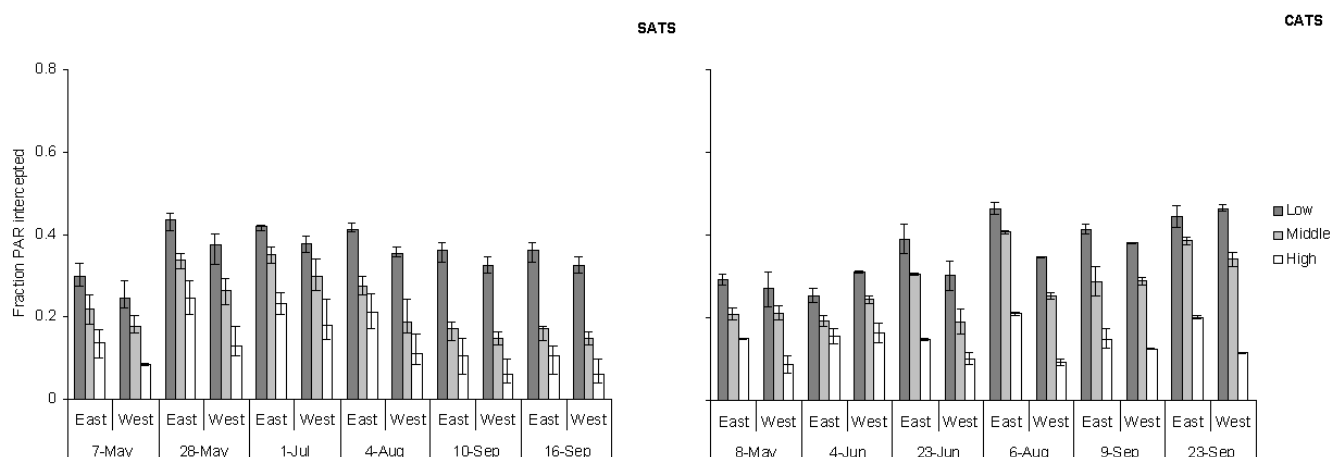
Figure 3.4. Fraction PAR intercepted by the spindle- (SATS) and columnar (CATS) apple tree system (average over the different plots) per side of the plot (east and west) from flowering till right after harvest, depicted per apple tree system for each measurement height (low, middle and high). Measurements were done approximately once a month (from flowering till right after harvest), three times during a day during diffuse- and five times during a day during direct light conditions. Except for the third and the fourth measurement, which were done during homogeneous direct light conditions, the measurements were conducted during homogeneous diffuse light conditions. The ranges depict the highest and lowest fraction of PAR intercepted measured within the different plots (three plots for the SATS, and two for the CATS), describing the variability in PAR interception between the different plots.

3.2 Destructive Measurements

3.2.1 Leaves

The specific leaf area (SLA)(cm^2 leaf area/g leaf dry weight) of both the SATS and the CATS decreased from flowering till right after harvest (Figure 3.5). Despite the SLA at the fourth measurement, where the SLA of the SATS was higher than the SLA of the CATS, the decreasing trend of both apple tree systems seems similar. No difference in fraction dry weight (g dry weight/ g fresh weight) of the leaves between both apple tree systems was found.
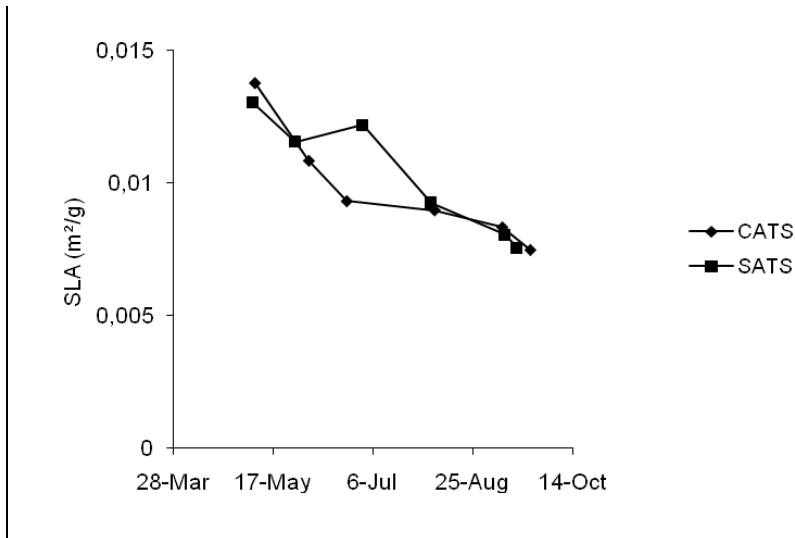
Figure 3.5. Specific leaf area (m^2 leaf area/g leaf dry weight) of the spindle- (SATS) and columnar apple tree system (CATS), determined approximately once a month from flowering till right after harvest. Per measurement in time, the number of leaves per plot were: 2324, 2668, 3029, 2896, 2632 and 2952 for the SATS and 1276, 1487, 2480, 2390, 1984 and 2011 for the CATS.

The leaf area index (m^2 leaf area/ m^2 surface area) increased until the fourth measurement (4 and 6 August for the SATS and the CATS respectively) for both apple tree systems (Figure 3.6). The CATS had a higher LAI than the SATS during the whole growing season and also increased faster. From flowering till right after harvest, the LAI of the CATS increased from 1.99 to 3.89 (increase of 1.90) versus an increase of 1.08 in LAI (from 1.44 to 2.52) for the SATS.
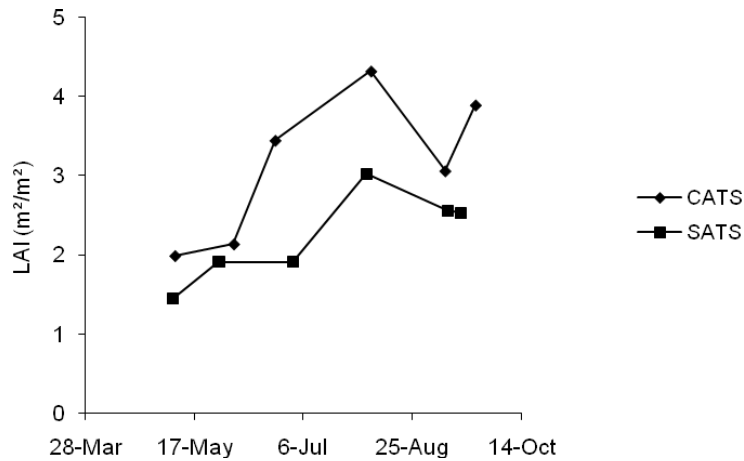
Figure 3.6. Leaf area index (m^2 leaf area/m^2 surface area) of the spindle- (SATS) and columnar apple tree system (CATS), determined approximately once a month from flowering till right after harvest. Per measurement in time, the number of leaves per plot were: 2324, 2668, 3029, 2896, 2632 and 2952 for the SATS and 1276, 1487, 2480, 2390, 1984 and 2011 for the CATS.
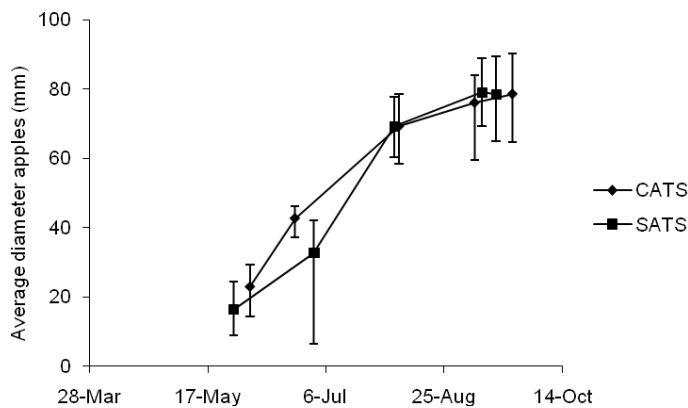
3.2.2 Apples

The average apple diameter of both tree systems increases from flowering till right after harvest, whereas there is almost no difference in apple diameter between the SATS and the CATS (Figure 3.7).

Figure 3.7. Average diameter (mm) of the columnar- (CATS) and spindle apple tree system (SATS), determined approximately once a month from about a month after flowering until harvest. The ranges represent the smallest and largest diameter in the plot per measurement. Per measurement in time, the total number of apples present per plot were: 73, 88, 108, 97 and 62 for the SATS and 37, 33, 35, 35 and 28 for the CATS.

However, compared to the CATS, the apple dry weight of SATS seems larger (Figure 3.8). The final dry weight yield of the CATS is 4.5 ton/ha versus 5.1 ton/ha for the SATS. This corresponds with 34.4 ton/ha and 33.2 ton/ha fresh weight respectively (see Figure VII.2 of

Appendix VI). Hence the apples of the CATS have a smaller dry weight fraction (g dry weight/g fresh weight); on average 0.11 versus 0.15 for SATS.
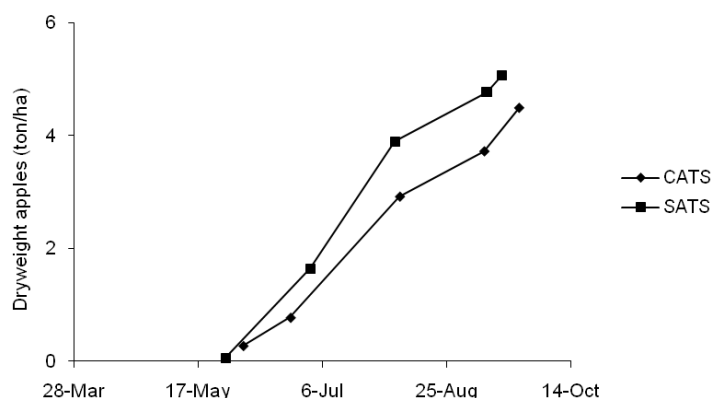
Figure 3.8. Dry weight apple yield in ton/ha for the spindle- (SATS) and columnar (CATS) apple tree system, determined approximately once a month from about a month after flowering until harvest. . Per measurement in time, the total number of apples present per plot were: 73, 88, 108, 97 and 62 for the SATS and 37, 33, 35, 35 and 28 for the CATS.
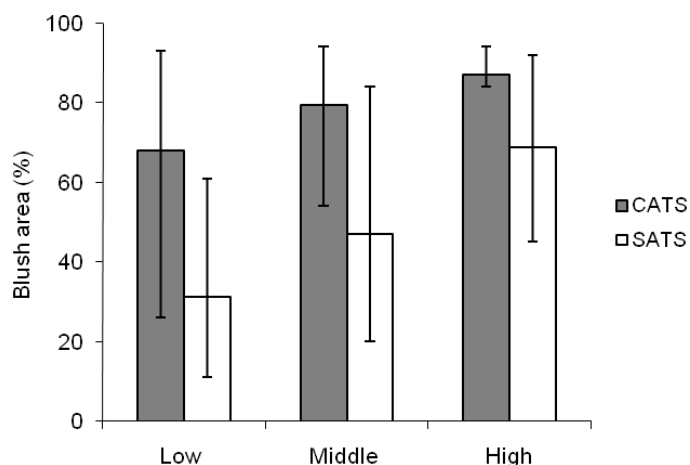
The blush area of both systems increased from apples low in the tree canopy to apples high in the tree canopy. The increase was largest for the SATS (increase of 37.4% blush area, compared to an increase of 19.0% blush area for the CATS), whereas the apples of the columnar tree had the largest blush area overall (Figure 3.9).

Figure 3.9. Average blush area (% blush on total apple surface) of the spindle- (SATS) and columnar (CATS) apple yield. The blush area was determined after harvest for all apples picked between the low and middle measurement height (low), between the middle and high measurement height (middle) and above the high measurement height (high). Per measurement in time, the total number of apples present per plot were: 73, 88, 108, 97 and 62 for the SATS and 37, 33, 35, 35 and 28 for the CATS. The ranges represent the highest and lowest blush area measured.

3.3 Apple production efficiency

In obtaining the results presented in this paragraph, it was assumed that the relation between each measurement (PAR interception and dry weight apples) over time was linear.

Hence, the relation between the cumulative amount of PAR intercepted (10^6 MJ/ha) and the cumulative dry weight yield of the apples (ton/ha) becomes linear for both apple tree systems (see Figure 3.10). However the slope of the line is steeper for the SATS, indicating more dry weight apple production per unit PAR intercepted (apple production efficiency) for the SATS than the CATS. The average apple production efficiency over time is 1.71 for the SATS and 1.19 ton dry weight apples $\cdot$ 10^6 MJ PAR^{-1} for the CATS.
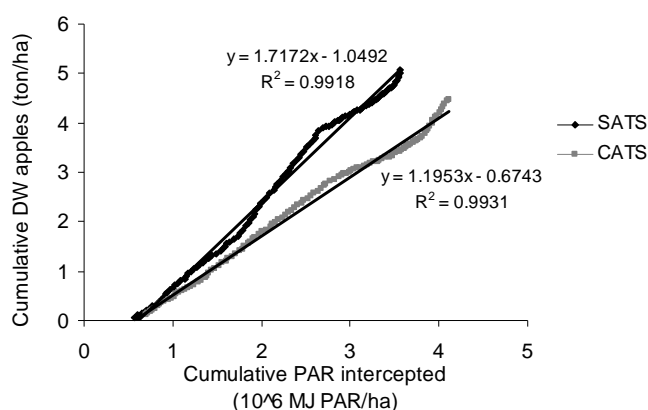
Figure 3.10. Relation between the cumulative amount of PAR intercepted (10^6 MJ PAR/ha) and the cumulative apple dry weight (ton/ha) of the spindle- (SATS) and the columnar (CATS) apple tree system, if was assumed that the relation between the different PAR interception- and apple dry weight measurements over time was linear.
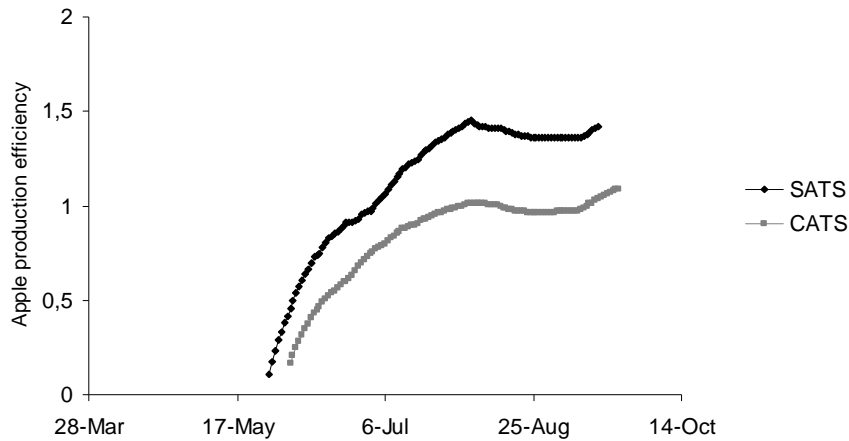
The relation between the cumulative fresh weight of the apples (ton/ha) and cumulative amount of PAR intercepted (10^6 MJ PAR/ha) was also linear, when the previous mentioned assumption was taken into account (see Figure VI.3 in Appendix VI). The fresh weight apple production per unit PAR interception was slightly higher for the SATS (11.40 for the SATS versus 9.50 for the CATS, with R^2 is 0.99 and 0.97 respectively) .

Over time the apple production efficiency (dry weight apples/ cumulative amount of PAR intercepted) was depicted in Figure 3.11. During all measurements the apple production efficiency of the SATS is higher than the CATS. For both apple tree systems the apple production efficiency is increasing until the beginning of August, from where the value more or less stabilizes (Figure 3.11).

Figure 3.11. Apple production efficiency (dry weight apples (ton/ha) produced per cumulative amount of PAR intercepted (10^6 MJ/ha)) over time for the spindle- (SATS) and columnar (CATS) apple tree system, if was assumed that the relation between the different PAR interception- and apple dry weight measurements was linear.

The relation between PAR interception and LAI was depicted in Figure 3.12, when was assumed that the relation between each measurement (PAR interception and dry weight apples) over time was linear. The PAR interception of both apple tree systems increases with an increasing LAI until a certain LAI value which is larger for the CATS than the SATS. From this value onwards PAR interception decreases.

Cumulative PAR intercepted
(10^6 MJ PAR/ha)

Figure 3.11. Relation between leaf area index (LAI) and the cumulative amount of PAR intercepted (10^6 MJ/ha)) for the spindle- (SATS) and columnar (CATS) apple tree system, if was assumed that the relation between the different PAR interception- and apple dry weight measurements was linear.
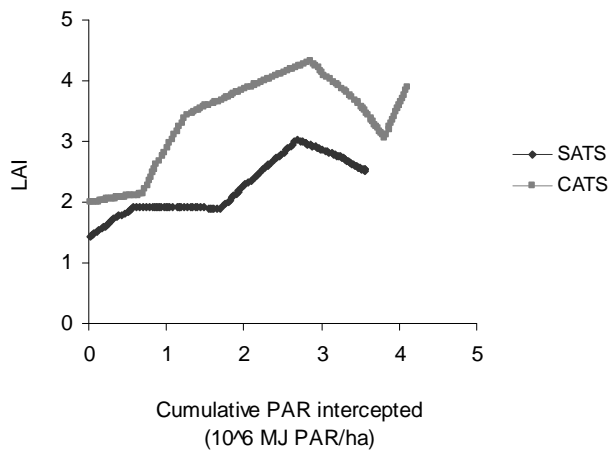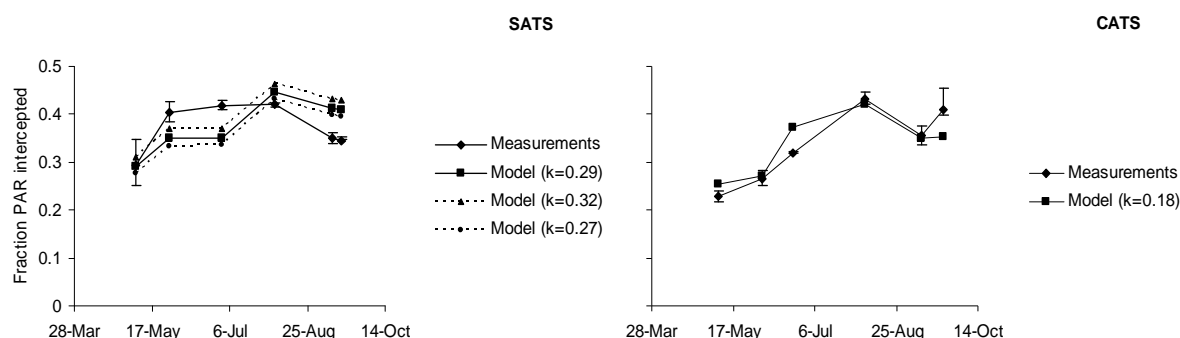
3.4 Model PAR interception

For the SATS the value for k, which was used as input in the model ROWCROP, was found to be 0.29 (see Figure 3.12). The variability of k was between 0.27 and 0.32 when respectively

the lower and upper boundary of variability in PAR interception between the plots during the measurements were used (depicted by the ranges in Figure 3.12, SATS, Measurements) .

The largest discrepancy in the trend of PAR interception over time between the model and the measurements is between the third and the fourth measurement (4 August and 10 September for the SATS, and 6 August and 9 September for the CATS). Before the fourth measurement PAR interception calculated by the model is lower than the PAR interception measured, however from the fourth measurement onwards this becomes the other way around.

For the CATS the trend of fraction PAR intercepted over time calculated by the model and measured was much more similar compared to the SATS, when k=0.18 was used as input. Furthermore, no variability for k (using two decimal places) was found when using the upper and lower boundary of variability in PAR interception between the different plots (represented by the ranges in Figure 3.12, CATS, Measurements).

Right after harvest the fraction PAR intercepted calculated via ROWCROP was 0.30 and 0.37 (versus the measurement results; 0.35 and 0.41) for the SATS and the CATS respectively. Average over the growing period the fraction PAR intercepted by the SATS and the CATS was 0.31 and 0.30 (versus the measurement results 0.37 and 0.34) respectively.

Figure 3.12 Fraction PAR intercepted by the spindle- (SATS) and columnar (CATS) apple tree system, measured beneath the tree canopy from flowering to just after harvest, and modeled via ROWCROP. For the SATS k=0.29 was used as model input, whereas the variability of k was found to be between 0.27 and 0.32 if respectively the lowest and highest fraction PAR intercepted measured within the different plots per measurement (depicted by the lower and upper values of the ranges in the measurement line) was used as a reference. For the CATS k=0.18 was used as model input, whereas no variability was found in k using two decimal places.

In Figure 3.13, the difference between the fraction PAR intercepted calculated by ROWCROP (using k=0.29 and k=0.18 as model input for the SATS and the CATS respectively) for both apple tree systems was shown. According to ROWCROP the fraction PAR intercepted by the CATS is lower than the fraction PAR intercepted by the SATS during the whole growing season, except at the third measurement (1 July for the SATS and 23 June for the CATS).
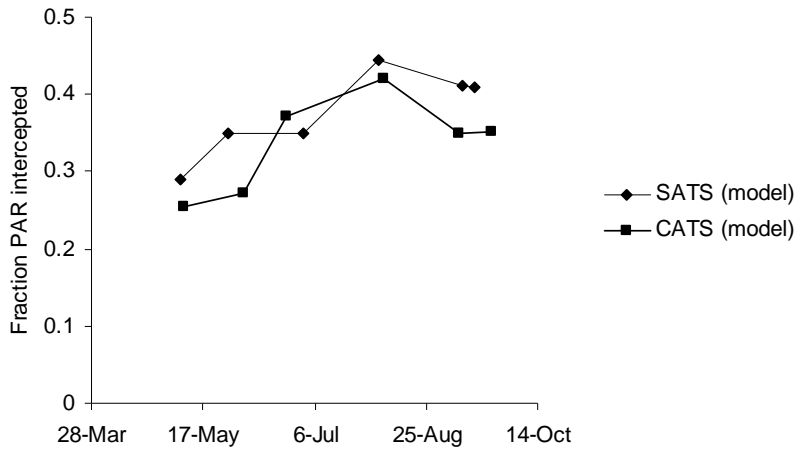
Figure 3.13 Fraction PAR intercepted from flowering till right after harvest by the spindle- (SATS) and columnar (CATS) apple tree system, calculated via the model ROWCROP.

According to ROWCROP, the fraction PAR intercepted by the SATS when the average LAI (2.23) and tree height (2.45m) were used, was 0.38 (Table 3.1; Default). When the default tree spacing was adjusted while the tree height and LAI were maintained, the maximum fraction PAR intercepted by the SATS was 0.46 (Table 3.1; Situation A). This fraction PAR intercepted was achieved when the smallest possible rectangular spacing was used (p=0.80 and w=0.80). If was assumed that the LAI increases linearly with the tree height and the tree becomes maximally 5m high towards its adult life phase (h=5. and LAI=4.55), the fraction PAR intercepted by the SATS with the default tree spacing becomes 0.61 (Table 3.1; Situation D). Using the latter tree height and LAI and the optimal rectangular tree spacing of 0.80m, the fraction PAR intercepted by the SATS calculated by ROWCROP becomes 0.71 (Table 3.1; Situation E). However, this tree spacing and height is not realistic when the currently available orchard machinery was used. Then the path width should be minimal 2.00m, the row height maximal 4.00m or 5.00m. The optimal tree spacing in these cases is 2.00x2.00m, which results in a fraction PAR intercepted of 0.60 if the tree height was 4m and 0.68 if the tree height was 5m (Table 3.1; Situation G and K). When this optimal realistic tree spacing was used as input into ROWCROP in combination with the default tree height and LAI, the fraction PAR intercepted by the SATS was 0.44 (Table 3.1; Situation B).

Table 3.1 Fraction PAR intercepted by the spindle apple tree system using different tree spacings, tree heights and leaf area indices. The bold values are different from the default inputs.

	h	p	r	LAI	k	Fraction PAR intercepted
Default	2,45	3,25	0,8	2,23	0,29	0,38
Situation A	2,45	**0,8**	0,8	2,23	0,29	0,46
Situation B	2,45	**2**	0,8	2,23	0,29	0,42
Situation C	2,45	**2**	**2**	2,23	0,29	0,44
Situation D	**5**	3,25	0,8	**4,55**	0,29	0,61
Situation E	**5**	**0,8**	0,8	**4,55**	0,29	0,71
Situation F	**5**	**2**	0,8	**4,55**	0,29	0,66
Situation G	**5**	**2**	**2**	**4,55**	0,29	0,68
Situation H	**4**	3,25	0,8	**3,64**	0,29	0,53
Situation I	**4**	**0,8**	0,8	**3,64**	0,29	0,63
Situation J	**4**	**2**	0,8	**3,64**	0,29	0,58
Situation K	**4**	**2**	**2**	**3,64**	0,29	0,60

Using the default inputs (average values for tree height, path width, row width and LAI) for the CATS in ROWCROP results in a fraction PAR intercepted of 0.34 (Table 3.2; Default). The maximum fraction PAR intercepted which could be achieved by adjusting the tree spacing to the smallest possible rectangular spacing (p=0.30m and r=0.30m) was 0.41 according to the model (Table 3.2; Situation A). Assuming that the LAI increases linearly with the tree height and the tree becomes maximally 5m high towards its adult life phase (h=5. and LAI=7.43), the fraction PAR intercepted by the CATS with the default tree spacing becomes 0.62 (Table 3.2; Situation D). Using the latter tree height and LAI and the optimal rectangular tree spacing of 0.80m, results in a fraction PAR intercepted of 0.73 for the CATS according to ROWCROP (Table 3.2; Situation E). However, this tree spacing and height is not realistic when the currently available orchard machinery has to be used. Then the path width should be minimal 2.00m, the row height maximal 4.00m or 5.00m and the row width minimal 2.00m. The optimal tree spacing in these cases is 2.00x2.00m, which results in a fraction PAR intercepted of 0.61 if the tree height was 4m and 0.69 if the tree height was 5m (see Table 3.2: Situation G and K). Furthermore there could be some doubt on how realistic and effective an LAI of 4.00m is.

Table 3.2 Fraction PAR intercepted by the columnar apple tree system using different tree spacings, tree heights and leaf area indices. The bold values are differ from the default inputs.

	h	p	R	LAI	k	Fraction PAR intercepted
Default	2,02	2,5	0,3	3	0,18	0,34
Situation A	2,02	**0,3**	0,3	3	0,18	0,41
Situation B	2,02	**2**	0,3	3	0,18	0,35
Situation C	2,02	**2**	**2**	3	0,18	0,38
Situation D	**5**	2,5	0,3	**7,43**	0,18	0,62
Situation E	**5**	**0,3**	0,3	**7,43**	0,18	0,73
Situation F	**5**	**2**	0,3	**7,43**	0,18	0,65
Situation G	**5**	**2**	**2**	**7,43**	0,18	0,69
Situation H	**4**	2,5	0,3	**5,94**	0,18	0,55
Situation I	**4**	**0,3**	0,3	**5,94**	0,18	0,65
Situation J	**4**	**2**	0,3	**5,94**	0,18	0,57
Situation K	**4**	**2**	**2**	**5,94**	0,18	0,61

3.5 Potential yield estimate CATS

Jacob (2004) stated that column apple varieties will allow a yield leap up to 150 tons of fresh weight per hectare, whereas SATS now yield about 60 ton ha^{-1} (Tromp *et al.*, 2005). In this paragraph a rough estimate of the potential yield of the CATS was made in order to test if a yield of 150 tons of dry weight is potentially achievable.

It was assumed that spindle apple trees (Elstar/M9) partition 60% of its dry weight into the fruit, 25% into the wood and 15% into the leaves, adapted from Wagenmakers (1996), Palmer *et al.*(2002) and Wagenmakers and Callesen (1995). Furthermore, it was assumed that the maximal (fresh weight) yield of the SATS in its adult phase could maximally become 70 ton/ha. This is about twice the fresh weight yield of the two year old SATS (33 ton/ha) measured during this research. In addition the dry weight fractions 0.11 and 0.15 were used for the CATS and the SATS respectively. The CATS is expected to partition less of its dry weight to the wood since it has less branches, which contributes to the partitioning to the fruit (Ruess, 2008). If It was assumed that the columnar trees have no branches and partition only 5% into wood for the stem and the roots, the partitioning into the apples and leaves becomes 80% and 15% respectively. Using the same maximal

yield increase (2.12 times the yield in the second year) as the SATS from the second year of growth to the adult growth phase, this results in a maximal fresh weight yield of 96 ton/ha. The latter rough maximal potential yield estimate does not correspond with the 150 ton/ha which Jacob (2004) claims.

4. DISCUSSION

The optimal tree spacing mentioned in the aim of this study was defined by the optimal fraction PAR interception, which was claimed to be 0.70 (Tromp *et al.*, 1996; Verheij and Verwer, 1973; Wagenmakers and Callesen, 1995; Wagenmakers and Tazelaar, 1999). The latter fraction PAR interception was not achieved by the SATS as well as the CATS (maximal 0.42 and 0.43 respectively (Figure 3.1), from flowering till right after harvest) according to the measurements as well as the model ROWCROP (Tables 3.1 and 3.2). It was expected that the optimal fraction of PAR was not intercepted by both apple tree systems yet, since both systems are still not in their adult phase of life. Wagenmakers and Callesen (1995) found 61% PAR interception for the Elstar/M9 (the effect of tree height on PAR interception was not significant) with a more or less similar tree spacing (3.00x1.00m) as the SATS used in this thesis. This might indicate that even the adult SATS can hardly achieve 70% PAR interception using approximately a 3:1 tree spacing, which was supported by the model ROWCROP (Table 3.1). Furthermore nowadays the way of pruning is more open compared to about 15 years ago when Wagenmakers conducted her research, which might contribute to the lower PAR interception found in this thesis.

If it was assumed that the LAI increases linearly with tree height, the fraction PAR interception by the SATS would be 0.53 and 0.61 for 4 and 5m high spindle trees respectively at the default tree spacing (p=3.25 and r=0.8m). This corresponds approximately with a 10% increase in light interception per meter increase of tree height (Wagenmakers *et al.*, 2001). However, the LAI at these heights was accordingly 3.64 and 4.55 respectively, which is larger than the optimal LAI between 3 and 4 claimed by Wagenmakers (1991), Wagenmakers and Callesen (1995) and Verheij and Verwer (1973). When the previously mentioned assumption was taken into account the tree heights at LAI 3 and 4 were 3.3 and 4m respectively, which results in a fraction PAR interception of 0.47 and 0.56 by the SATS according to ROWCROP. According to the model the SATS is hence not able to intercept 70% of PAR with the optimal LAI. The relation between LAI and amount of PAR intercepted (10^6 MJ) has a more or less exponential trend, as was found in Wagenmakers and Callesen (1995). However, the same LAI intercepted less PAR for both apple tree systems compared to the findings of Wagenmakers and Callesen (Figure 3.11).

In line with the results of Jackson and Palmer (1971) and Wagenmakers and Callesen (1995), rectangular tree spacings (similar path- and row width) is most beneficiary for total light interception. The smallest rectangular tree spacings possible for SATS and CATS (0.80x0.80m and 0.30x0.30m respectively) hence intercepted the largest fraction PAR. However the light distribution within the canopy might be negatively influenced by these small rectangular tree spacings (Wagenmakers *et al.*, 2001). Furthermore, considering the currently used machinery in orchards, the path width should be minimally 2m in order to allow tractors driving through. Again with the rectangular tree spacing (2mx2m) results

in the largest fraction PAR intercepted. Using this tree spacing (when was assumed that the LAI increases linearly with the tree height) at 4 and 5m tree height the fraction PAR intercepted determined by ROWCROP was 0.60 and 0.68 for the SATS and 0.61 and 0.69 for the CATS respectively.

The decrease in PAR interception from August onwards is hard to explain (Figure 3.1). The fact that the increase in PAR interception stops is clear because the leaves are fully grown by then (Wagenmakers and Callesen, 2005). Accordingly the LAI shows approximately the same trend as PAR interception over time; increase till August (while the leaves are still growing) and afterwards a decrease (Figure 3.6). However, after this point it was expected that the fraction PAR intercepted as well as the LAI would stabilize, since no leaves are falling down or pruning is being conducted. The small difference between the PAR interception before and after harvest indicates that the apples hardly affect PAR interception in contrast to the leaf area. Overall the LAI was during the growing season larger for the CATS than the SATS, while the fraction PAR intercepted is until August higher for the SATS. The leaves of both apple tree systems furthermore became thicker during the growing season (Figure 3.5). The leaves which were produced later in the growing season might have been structurally thicker.

The fraction PAR intercepted measured in the canopy (middle and high measurement heights) was lower than the fraction PAR intercepted measured underneath the tree canopy (Figure 3.1 and 3.2). Obviously at higher measurement heights less leaf area was available for intercepting PAR, which explains this result (Wagenmakers en Callesen, 1995). The larger differences between the PAR interception at these measurement heights for the CATS is a characteristic of the tree shape. The assumption of the same leaf area per canopy volume, which was used in order to calculate the measurement heights, seems to be fairly reliable. However, for the CATS the difference in PAR interception per measurement height was more evenly distributed. This might have to do with the fact that the spindle tree shape is more complex because of the larger branches, which makes the distribution of LA per canopy volume less homogeneous.

The time of day had an influence on the fraction PAR intercepted, especially for the CATS under direct light conditions (Figure 3.3). This finding was supported by Wünsche *et al*. (1995) who found that PAR interception could be best measured during homogeneous diffuse light conditions, since then the variations in PAR interception over the day were small. Furthermore, in this article it was proven that the effect of time of day on PAR interception was most pronounced for more vertical canopies which emphasises the importance of several readings a day. This was the reason why five instead of three PAR interception measurements during the day were conducted under direct light conditions.

Also differences in PAR interception at each side of the row (east/west) were found (Figure 3.4). This indicates that the row shape is not homogeneous. Therefore it was very important to distribute the plot size over the east and the west side of the row (Appendix I). The row at the east side of the CATS row measured, was higher than the CATS row. This

could have contributed to higher interception values for the east row side of the CATS, especially later on in the season. However, since no clear trend of higher PAR interception at the east side of the row was found for the CATS, it seems likely that there was no large effect of the higher east neighbour row on PAR interception.

In most cases during PAR interception measurements the SunSan Analysis System gave a small negative value for PAR interception when PAR interception was expected to be very low (e.g. measured at the high measurement height). The first possible reason which comes in mind was that the reference sensor received shade. However, this was carefully watched during the measurements, and before the measurement of each plot the difference between PAR intercepted by the SunScan probe and the BFS was determined which allowed for correction of this difference during the analysis of the data. Furthermore, in order to find the cause of the negative values the PAR interception measured by the SunScan Analysis System was compared to the values intercepted with another light measurement tool; which showed no difference. The negative values were treated as missing values during the data analysis.

The increase in apple diameter is almost similar for both apple tree systems over time (Figure 3.7). This increase corresponds with an increase in apple dry weight. However, the increase is larger for the SATS than the CATS (Figure 3.8), indicating that the apple production efficiency over time (Figure 3.10 and 3.11) is larger for the SATS than the CATS. So the SATS is able to produce more apple dry weight per unit PAR intercepted with a smaller LAI. The different cultivars and rootstocks used will be mainly affecting this. Although the fraction dry weight is higher for the SATS, the same conclusion can be drawn as the latter in combination with fresh instead of dry weight.

Even if 80% dry matter partitioning into the fruits was used in calculating the potential yield of the CATS, the potential yield estimate (96.12 ton/ha) does not even come close to the potential yield of 150 ton ha^{-1} calculated by Jacob (2004). While dry matter partitioning into the fruits of 80% is already large compared to 55% for Golden Delicious/M9 and 65% for Crispin/M27 (Palmer *et al.*, 2002). Even under New Zealand circumstances, which are known to be more favorable, the highest percentage of dry weight partitioned into the fruit was 70% for Breaburn and Fuji (Palmer *et al.*, 2002). Moreover harvest indices over 70% are rarely sustainable due to the risk of biennial bearing (Palmer *et al.*, 2002; Wagenmakers and Callesen, 1995). In addition McIntosh/MM106,which is the variety from which the CATS were developed via mutation and crosses, partitions only 33% of its dry matter into the fruits (Palmer *et al.*, 2002). Accordingly, reasons to think that a smaller fraction dry weight partitioned into the fruit is more realistic. This would however even enlarge the gap between the potential yield estimate conducted in this research compared to the 150 ton ha^{-1} claimed by Jacob (2004).

The blush area of the apples was overall higher for the CATS, however the increase in blush area from low to high in the tree canopy and the variability per measurement height was larger for the SATS (Figure 3.9). The latter was to be expected since the tree shape of the SATS allows less light in the inner part of the canopy which contributes to the cause of the lower blush area compared to the CATS. The higher in the spindle tree, the smaller becomes this effect, since the tree canopy higher in the tree becomes less wide. However since two different varieties were used in this study (Elstar/M9 and Suncats/MM111) it is hard to compare the exact blush area values for both apple tree systems. The blush area of one variety which is optimal in terms of marketability for this variety, does not necessarily have to be the same for the other variety. However, this study aimed to compare to different apple tree systems, which in this case by definition involved different varieties.

The apple tree systems studied were both two year old. Considering practice however, the adult apple tree systems are more interesting since the trees are in this most yielding stage the largest time of their lives. The relation between the two year old apple tree systems and adult apple tree systems concerning PAR interception is not investigated yet. Moreover, this relation could vary between the two apple tree systems, since two different varieties on different rootstocks (Elstar/M9 and Suncats/ MM111) were used. There are for example some indications that certain varieties of the columnar apple tree system may suffer more from (total or partial) biennial bearing (Ruess, 2000). This would certainly influence the fruit production efficiency over the years. Furthermore, if one variety for instance would develop more slowly compared than the other. This would complicate comparison of the two apple tree systems when they are not adult yet. As from this study only conclusions could be drawn of the two year old spindle- and columnar apple tree systems, further research using adult apple tree systems is recommended.

The columnar- and spindle apple tree systems used in this study were not located at the same place in the Netherlands; Wognum (longitude 5.03 °, latitude 52.68 °) versus Randwijk (longitude 5.71°, latitude 51.94 °) the Netherlands respectively. This might have an influence on the PAR interception measurements, since the sun is directed slightly different on different latitudes. For example Elstar might receive 30% more light in New Zealand compared to the Netherlands, because of the higher levels of incident light in New Zealand (Wagenmakers 2001). However, since both locations used during this research are in the Netherlands and the row direction within the orchard was north-south for both apple tree systems at both locations, this influence was neglected.

5. CONCLUDING REMARKS

This study aimed to obtain the optimal tree density and spacing of two year old columnar- (Suncats/ MM111) versus spindle apple tree systems (Elstar/ M9) by measuring and modelling their light interception and fruit production efficiency (dry weight yield per unit of PAR intercepted).

The optimal tree density and spacing was defined as the plant spacing at which 70% of the available amount of PAR is intercepted by the canopy. In general can be concluded that 70% PAR interception is hardly achievable for both apple tree systems. Especially if the size of the currently used orchard machinery is taken into account in determining the tree spacing.

Only when it was assumed that the LAI increased linearly with tree height, the optimal fraction PAR intercepted of 0.70 could be achieved when the trees were 5.00m high according to the model ROWCROP (using 0.29 as input value for the extinction coefficient k) and the path- and row width were both 0.80m. In reality the path width should be minimally 2m in order to allow the current machinery used in orchards to go through the row. The highest fraction PAR intercepted for the SATS using this path width was 0.68 (h=5.00m, p=2.00m, w=2.00m and LAI=4.55). Using the default tree spacing (p=3.25m and w=0.80m) 0.61 was the highest fraction PAR intercepted possible (h=5m, LAI=4.55).

The tree spacing at which the highest fraction PAR was intercepted for the CATS was also rectangular: p=0.30m and w=0.30m. Only when it was assumed that the LAI increased linearly with tree height, the optimal fraction PAR intercepted of 0.70 could be achieved when the trees were 5m high according to ROWCROP (using 0.18 as input value for the extinction coefficient k). When the realistic path width of 2.00m was fixed, the best row width in order to intercept the largest amount of PAR was 2.00m. Taking into account the previously mentioned assumption, if the trees become 5.00 or 4.00m high the fraction PAR intercepted by the CATS (p=2.00m, r=2.00m) was 0.69 or 0.61 respectively. Using the default tree spacing (p=2.5 and w=0.3) 0.62 was the highest fraction PAR intercepted possible (h=5.00m, LAI=4.55).

The total fraction PAR intercepted by the SATS and the CATS (measured below the tree canopy) increased from flowering till right after harvest. The increase was larger for the CATS (from 0.23 to 0.41) than for the SATS, which resulted in a slightly higher fraction PAR intercepted by the CATS (from 0.29 to 0.35) right after harvest. This is in line with the faster increase of LAI of the CATS (from 1.99 to 3.89) compared to the SATS (from 1.44 to 2.52). However, the CATS started off (until August) intercepting less PAR than the SATS, while the LAI of the CATS was higher compared to the LAI of the SATS during the whole

growing season. As well as the PAR interception over time, the LAI seemed to have a maximum value after which PAR interception decreases (about 4 for the CATS and 3 for the SATS).

The fraction PAR intercepted at the low measurement height was highest, followed by the fraction PAR interception found at the middle and high measurement heights, respectively. The similar trend for each measurement height and both apple tree systems supports the assumption of the same leaf area per canopy volume. The trend in PAR interception for each measurement height is increasing until August from where the fraction PAR intercepted decreases for both apple tree systems.

At each measurement height, differences in PAR interception between the measurement times on a day were observed. These differences were similar for each measurement height per measurement. For the CATS the PAR interception measurements done at 10.00h were always lowest and at 16.00h almost always highest. In addition the variability between measurement times during a day was larger during direct light conditions, which indicates the importance of measuring several times during a day (more than during diffuse light conditions).

PAR interception differed also for both apple tree systems and measurement heights for each side (east/west) of the row. For the CATS these differences were largest during direct light conditions, indicating that it is better to measure PAR interception during diffuse light conditions in order to get a more homogeneous result. And the east side of the row intercepts more light at each measurement height for SATS.

The specific leaf area (SLA) decreased from flowering till right after harvest, which means that the leaves became thicker during the growing season. Probably because the leaves which are initiated later on in the season were thicker than the leaves which were already starting to grow direct after flowering.

The apple diameter enlarged over time, which is in line with the increase in apple dry- and fresh weight for both apple tree systems. The dry weight yield at harvest was larger for the SATS (5.1 versus 4.5 ton/ha), while the final fresh weight yield was slightly higher for the CATS (34.4 versus 33.2 ton/ha for the SATS). Consequently, the CATS has a smaller dry weight fraction (0.11 versus 0.15g dry weight/g fresh weight for the SATS). The cultivar difference between the two apple tree systems will affect the size as well as the fraction dry weight and partitioning.

The blush area increased from apples low in the tree canopy to apples high in the tree canopy for both apple tree systems, indicating that the apples high in the tree canopy

intercept more light. The spindle tree shape ensures the largest difference in light interception of the apples between the low, middle and upper part of the canopy, since the increase in blush area was largest for the SATS. Also blush area will to a large extend be influenced by the cultivar difference between the two apple tree systems.

Apple production efficiency over time was larger for SATS (1.71 versus 1.19 for the CATS), assuming that the relation between the different PAR interception measurements and apple dry weight measurements was linear. This is in line with the higher PAR interception and apple dry weight of the SATS over time.

6. RECOMMENDATIONS FOR FURTHER RESEARCH

It would be recommendable to conduct a similar research also the coming years, in order to define if it is worthwhile for growers to plant columnar apple trees. Of course this does not only depend on PAR interception and apple production efficiency, but also on the marketability of the columnar apples and the costs involved for starting and maintaining such an orchard. Now only one column variety was used, but it would be worthwhile to see if the same conclusions can be drawn for other column varieties. In a following investigation it is important that the n (repeats) are higher to be able to draw statistically valid conclusions. This, along with different tree spacings and heights for each orchard system involves a more extended research plot. The different tree spacings and heights could verify the fraction PAR interception calculated via ROWCROP. The model ROWCROP could also be extended by defining the tree shape more exactly using L-systems. This would allow for visualising and more accurate calculation of PAR interception. It is important to conduct such an experiment during several years following the same trees as they grow older, whereas the adult life phase of the trees are most important. In this way certain tillage problems which may occur (e.g. pests, diseases, storage problems, biennial bearing) become known and can be used in defining if it is worthwhile for growers to plant columnar apple trees.

REFERENCES

Balkhoven-Baart, J.M.T., Wagenmakers, P.S., Bootsma, J.H., Groot, M.J., Wertheim, S.J., 2000. Developments in dutch apple plantings. *Acta Horticulturae*, 513: 261-269.

Gijzen,H. and Goudriaan, J., 1989. A flexible and explanatory model of light distribution and photosynthesis in row crops. *Agricultural and Forest Meteorology* 48: 1-20.

Goudriaan, J., 1977. Crop micrometeorology: a simulation study. Simulation monographs. Pudoc, Wageningen.

Jackson, J.E., Palmer, J.W., 1971. Interception of light by model hedgerow orchards in relation to latitude, time of year and hedgerow configuration and orientation. *Journal for Applied Ecology*: 341–357.

Jacob, H.B., 2004. http://www.campus-geisenheim.de/fileadmin/Forschungsanstalt/Gartenbau/ Obstbau/pdf-Dateien/englische_pdfs/CatsStory0806e.pdf, consulted at 17-01-2010.

Leffelaar, P.A. and Scholten, H.M., 2010. Course: "models for forest and nature conservation" (INF-31806). Group Information Technology, Wageningen University.

Palmer, J.W., Wünsche, J.N., Meland, M., Hann, A., 2002. Annual dry-matter production by three apple cultivars at four within row spacings in New Zealand. *Journal of Horticultural Science & Biotechnology,* 77(6): 712-717.

Potter E., Wood, J., Nicholl, C., 1996. SunScan Canopy Analysis System; User Manual SS1-UM-1.05. http://www.delta-t.co.uk/products.html?product2005092818906, consulted at 19-06-09.

Pronk A.A., Goudriaan, J., Stilma, E. and Challa, H., 2003. A simple method to estimate radiation interception by nursery stock conifers: a case study of eastern white cedar. *NJAS Wageningen Journal of Life Sciences,* 51(3): 279-295.

Ruess, F., 2008. Apfelsorten mit säulenwuchs – die rückkehr der superspindel? *Obstbau,* 8: 410-414.

Stilma, E., 2001. Description of conifer growth compared to roses supported by experimental research, with emphasis on radiation interception and water use efficiency. *MSc. Thesis, Wageningen University*, Wageningen: 22-27.

Tromp, J., Webster, A.D., Wertheim, S.J., 2005. Planting system and tree shape. *Fundamentals of Temperate Zone Tree Fruit Production,* 15: 190-198.

Verheij, E.W.M. and Verwer, F.L.J.A.W., 1973. Light studies in a spacing trial with apple on a dwarfing and a semi-dwarfing rootstock. *Scientia Horticulturae*, 1: 25-42.

Wagenmakers, P.S., 1991. Planting systems for fruit trees in temperate climates. *Critical Reviews in Plant Sciences,* 10: 369-385.

Wagenmakers, P.S., 1995a. General Introduction. In 'Light relations in orchard systems'. *PhD Thesis, Landbouwuniversiteit Wageningen*: 11-15.

Wagenmakers, P.S., 1995b. Light distribution in apple orchard systems in relation to production and fruit quality. *Journal of Horticultural Science,* 70 (6): 935-948.

Wagenmakers, P.S., Callesen, O. (1995). Light distribution in apple orchard systems in relation to production and fruit quality. *Journal of Horticultural Science,* 70 (6): 936-948.

Wagenmakers, P.S. (1996). Effects of light and temperature on potential apple production. *Acta Horticulturae,* 416: 191-197).

Wagenmakers, P.S., Tazelaar M. (1999). Modelling light interception on the basis of sunfleck measurements. *Acta Horticulturae,* 499: 297-303.

Wagenmakers, P.S., Bootsma, J.H., Groot, M.J. (2001). Orchard systems for apple and pear: conditions for succes. *Acta Horticulturae,* 557: 209-227.

Wünsche, J.N., Lakso, A.N., Robinson, T.L. (1995). Comparison of four methods for estimating total light interception by apple trees of varying forms. *HortScience,* 30 (2): 272-276.

Wünsche, J.N., Palmer, J.W. (1998). Comparison of non-destructive methods for estimating leaf area of apple tree canopies. *Acta Horticulturae,* 243: 175-184.

APPENDIX I. Plot size

All measurements were conducted in different plots within one orchard row. One plot should be a repetitive and representative unit within the orchard, in order to be able to extrapolate the results of the measurements to a larger surface area (ha^{-1}). The width (east-west direction) as well as the length of this unit was experimentally determined before the start of the actual experiment for the spindle apple tree system. A similar plot size, but adapted to the other tree system, was accordingly used for the columnar tree system (Chapter 2.2.1.2). The plot sizes for spindle and columnar trees do not have to be exactly the same, because the plot size will be recalculated to hectares in the end. However, the plot size has to be chosen in such a way that the variability in one series of plots in one system is less than the variability between systems.

By measuring PAR interception (as described in Chapter 2.2.1) at one side of the row (Figure I.1, a and b) and at two sides of the row (Figure 1, b and c) the width of the plot was determined, since the results of this experiment clarify whether or not it is justified to assume that both sides of the tree are similar at solar noon.

a   b   c   d
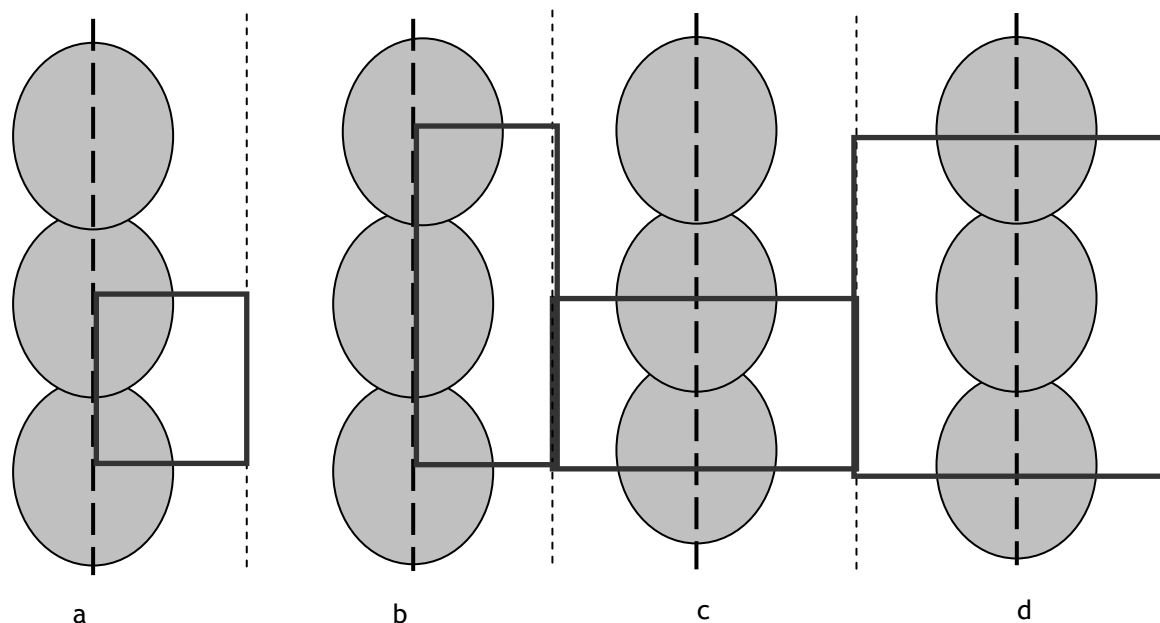
Figure I.1. Plot size of PAR measurements. The grey circles represent the spindle trees, whereas the thick dashed line shows the middle of the row and the thin dashed line the middle of the path. The square boxes (a, b, c and d) depict the different plot sizes which were used in order to define the right plot size to use for the PAR interception measurements.

The length of the plot (north-south direction) was determined by measuring PAR interception for different lengths in the row and checking the variance of the PAR interception (so for example checking the difference in PAR interception of the trees in the

square box in a and the square box in b in Figure V.1).
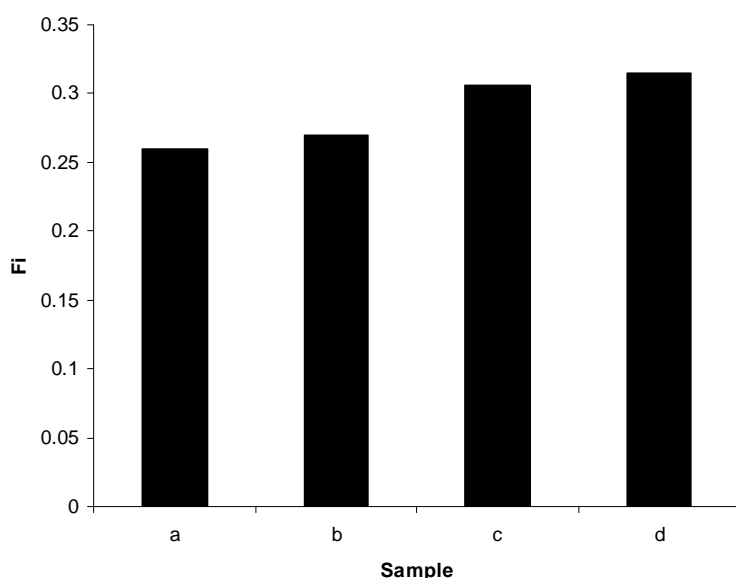
Figure I.2. Fraction PAR intercepted (Fi) of different plot sizes (a, b, c and d, according to Figure I.2).

Figure I.2 shows that there is only a small difference (approximately 1%) between the fraction PAR intercepted by the spindle trees between the two different plot lengths (a and b). However, the difference between the two plot widths is (a versus c and b versus d) is approximately 5%.

The latter result shows that it cannot be assumed that both sides of the tree are similar (east-west). So the plot should include half of the path width both at the east and at the west side. Since there was only a very small difference between the two plot lengths (a versus b and c versus d) the smallest plot length was chosen. Hence, plot size c as depicted in Figure I.1 was the final plot size.

In deciding on the number of plots and the number of measurements within these plots also the duration of the measurements were considered. One measurement (including the three replications) should not take longer than one hour, since otherwise the effect of the time of the day, will not be noteworthy anymore. This resulted in three plots in which four measurements (1m) and four extended measurements (0.625m), as is depicted and explained in Chapter 2.2.1.2.

A similar plot size was chosen for the columnar apple tree system, though adapted to the different system. The width of the plot includes half of the path width at the east and west side of the plot (since the path width of the two apple tree systems are different, the plot width is different). Furthermore, the length of the plot includes more trees than the plot of the spindle apple tree system, since the latter has more space between the trees and more trees of the same variety available. Also by determining the plot size of the columnar apple tree system, the duration of one measurement at a certain time including

the replications was no longer than 1h. The exact plot size of the columnar trees with additional information on the number of measurements within a plot can be found in Chapter 2.2.1.2.

APPENDIX II. PAR interception Beam Fraction Sensor versus SunScan Probe

The relation between the amount of PAR intercepted by the Beam Fraction Sensor and the amount of PAR intercepted by the SunScan Probe was tested by measuring the amount of PAR intercepted with the SunScan Probe and the incident PAR intercepted by the Beam Fraction Sensor while covering 0, 20, 40, 60, 80 and 100 cm of the SunScan Probe with non-light transmitting duct isolation under homogeneous light conditions. This resulted in a linear relation between the length of the active part of the SunScan Probe and the percentage of PAR intercepted with the SunScan Probe (Figure II.1).

$y = 0.9914x + 1.1262$

$R^2 = 0.9993$
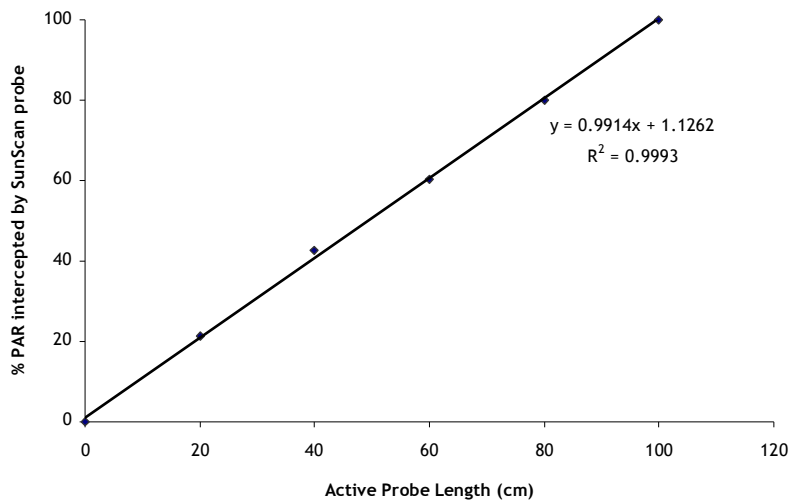
Figure II.1. Interception of photosynthetic active radiation when covering 0 to 100cm of the SunScan Probe with steps of 20cm from the tip of the probe in the open field under homogeneous direct light conditions. The active probe length is depicted on the y-axis and can be calculated by subtracting the length (cm) of the probe which is covered from the total probe length (100cm). The x-axis represents the % of PAR intercepted by the SunScan Probe.

APPENDIX III. Calculation PAR interception per plot

The SunScan Canopy Analysis System internally converts the PAR interception output into a flux with the unit µmol m^{-2} s^{-1} [a].

Spindle apple tree system

One PAR interception measurement plot consists of four measurements of 1m length (using the total active SunScan probe length) and four measurements using 0.625m of the active probe length (Figure III.1).
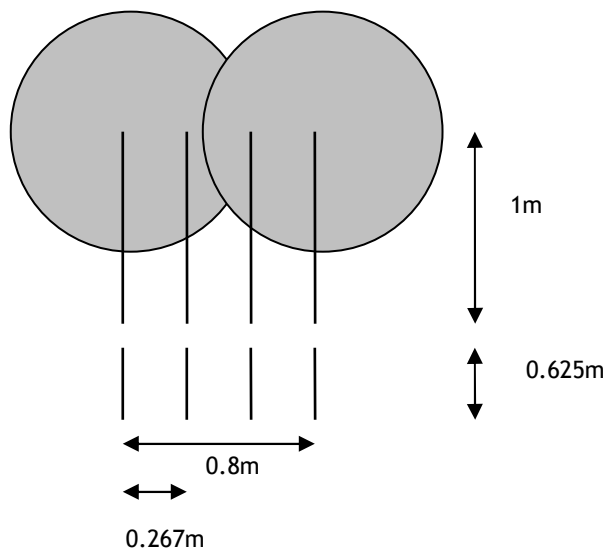
Figure III.1. Spatial arrangement of the PAR measurements of one plot within the spindle apple tree system. The grey circles represent the spindle trees, whereas the vertical lines represent the PAR measurements. Four PAR measurements were conducted with the total length of the SunScan Probe (1m) perpendicular to the row. The other four measurements were done while 0.375m of the SunScan probe was covered in order to be able to measure in total half of the path width (1.625m).

In order to calculate an average value for the PAR interception over the whole surface of the plot, the surface area was assigned to each measurement; (1m · 0.267m) and (0.625m · 0.267m) to the 1m measurement and the 0.625m measurement, respectively (see Figure III.1).

---

[a] Information on this conversion was not available in the manual of the system (Potter *et al.*, 1996[2]). Probably the SunScan probe receives PAR in µmol s^{-1} probe surface $^{-1}$. If there are 64 sensors with each a surface of 1.23 cm^2 (if diameter of SunScan Probe was 1.25 cm), the total sensor surface would be 78.54 cm^2. Per cm^2 the flux would accordingly be: y µmol (78.54 cm) $^{-2}$ * x. To calculate the flux per m^2, 10^4 cm^2 should be substituted for x. Accordingly the internal conversion factor of the SunScan Canopy Analysis System would be (10^4/78.54) m^{-2}.

If I_i is the radiation intensity below the plant canopy (µmol m^{-2} s^{-1}) and I_0 above the plant canopy (µmol m^{-2} s^{-1}), the PAR intercepted by the tree of the four measurement using 1m of the SunScan probe is:

$$\sum_{i=1}^{4} I_{0i}(1 \cdot 0.267) - I_i(1 \cdot 0.267)$$

The SunScan probe was covered over (1m-0.625m) 0.375m during the other four measurements. Still, the signal of the SunScan probe will have an intensity of I/0.625. Accordingly the PAR intercepted by the tree of the four measurements using only 0.625m of the active probe length is:

$$\sum_{i=5}^{8} I_{0i}(0.625 \cdot 0.267) - \frac{I_i}{0.625}(0.625 \cdot 0.267)$$

Hence, the average amount of PAR intercepted by one plot became:

$$\frac{\sum_{i=1}^{4} [I_{0i}(1 \cdot 0.267) - I_i(1 \cdot 0.267)] + \sum_{i=5}^{8} [I_{0i}(0.625 \cdot 0.267) - (I_i \cdot 0.267)]}{\sum_{i=1}^{4} (1 \cdot 0.267) + \sum_{i=5}^{8} (0.625 \cdot 0.267)}$$

Which can be simplified by deleting 0.276 to:

$$\frac{\sum_{i=1}^{4} [I_{0i} - I_i] + \sum_{i=5}^{8} [0.625 \cdot I_{0i} - I_i]}{4(1 + 0.625)}$$

In order to calculate the fraction of PAR intercepted by the tree, the amount of PAR intercepted by the tree should be divided by the total amount of PAR available:

$$\frac{\sum_{i=1}^{4} [I_{0i} - I_i] + \sum_{i=5}^{8} [0.625 \cdot I_{0i} - I_i]}{\sum_{i=1}^{4} I_{0i} + \sum_{i=5}^{8} 0.625 \cdot I_{0i}}$$

Columnar apple tree system

In the columnar apple tree system, one plot consists of seven measurements of 1m length (using the total active SunScan probe length) and seven measurements using 0.25m of the active probe length (Figure III.2).
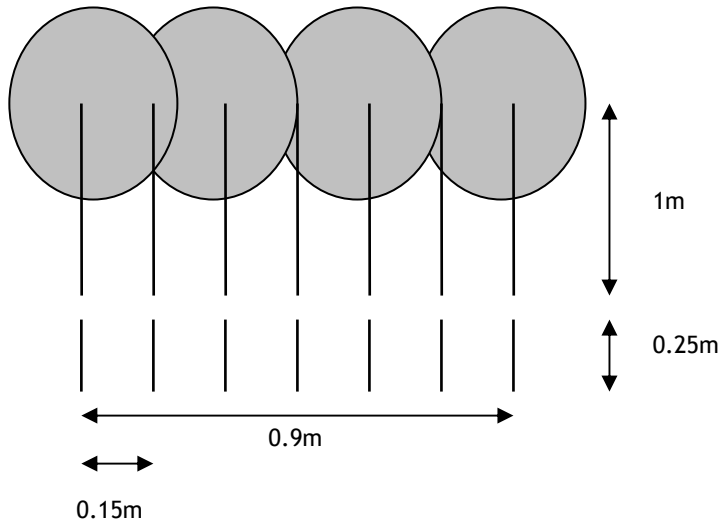
Figure III.2. Spatial arrangement of the PAR measurements of one plot within the columnar apple tree system. The grey circles represent the spindle trees, whereas the vertical lines represent the PAR measurements. Seven PAR measurements were conducted with the total length of the SunScan Probe (1m) perpendicular to the row. Seven other measurements were done while 0.25m of the SunScan probe was covered in order to be able to measure in total half of the path width (1.25m).

To each PAR interception measurement the linked surface was assigned; (1m · 0.15m) and (0.25m · 0.15m) to the 1m measurement and the 0.625m measurement, respectively. Hence, the amount of PAR intercepted (µmol m^{-2} s^{-1}) intercepted by the tree of the seven measurements using the total active SunScan probe length (1m) was:

$$\sum_{i=1}^{7} I_{0i}(1 \cdot 0.15) - I_i(1 \cdot 0.15)$$

During the other seven measurements the active probe length was only 0.25m. The intensity of the signal of the SunScan probe will be consequently *I/0.25*. Accordingly, the PAR intercepted by the tree of these seven measurements was:

$$\sum_{i=8}^{14} I_{0i}(0.25 \cdot 0.15) - \frac{I_i}{0.25}(0.25 \cdot 0.15)$$

Hence, the average amount of PAR intercepted by one plot becomes:

$$\frac{\sum_{i=1}^{7} [I_{0i}(1 \cdot 0.15) - I_i(1 \cdot 0.15)] + \sum_{i=8}^{14} [I_{0i}(0.25 \cdot 0.15) - (I_i \cdot 0.15)]}{\sum_{i=1}^{7}(1 \cdot 0.15) + \sum_{i=8}^{14}(0.25 \cdot 0.15)}$$
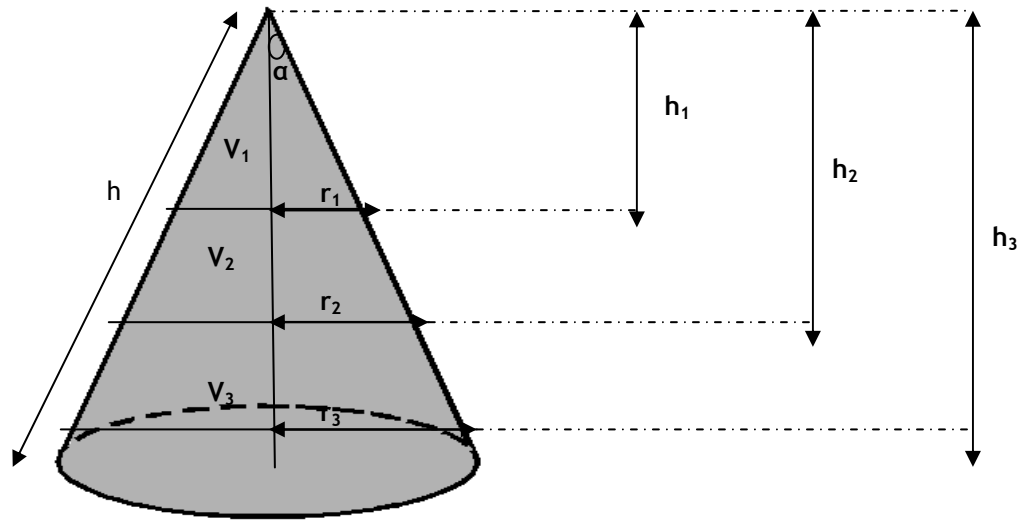
Which can be simplified by deleting 0.15 to:

$$\frac{\sum_{i=1}^{7} [I_{0i} - I_i] + \sum_{i=8}^{14} [0.25 \cdot I_{0i} - I_i]}{7(1 + 0.25)}$$

In order to calculate the fraction of PAR intercepted by the tree, the amount of PAR intercepted by the tree should be divided by the total amount of PAR available:

$$\frac{\sum_{i=1}^{7} [I_{0i}-I_i]+\sum_{i=8}^{14} [0.25 \cdot I_{0i}-I_i]}{\sum_{i=1}^{7} I_{0i}+\sum_{i=8}^{14} 0.25 \cdot I_{0i}}$$

APPENDIX IV. Determination measurement height in spindle canopy

Figure IV.1 Picture of the cone shaped canopy of the spindle tree with V_1, V_2, and V_3 representing the equal volumes of the upper, middle and lower part of the canopy respectively. Furthermore h_1, h_2 and h_3 represent the corresponding heights, r stands for radius, α represents the angle and H is the hypotenuse.

$$V_1 = \tfrac{1}{3} \cdot h_1 \cdot \pi \cdot r_1{}^2 \qquad\qquad \text{Equation IV.1}$$

$$V_2 = \tfrac{1}{3} \cdot h_2 \cdot \pi \cdot r_2{}^2 - \tfrac{1}{3} \cdot h_1 \cdot \pi \cdot r_1{}^2 \qquad\qquad \text{Equation IV.2}$$

$$V_3 = \tfrac{1}{3} \cdot h_3 \cdot \pi \cdot r_3{}^2 - \tfrac{1}{3} \cdot h_2 \cdot \pi \cdot r_2{}^2 \qquad\qquad \text{Equation IV.3}$$

$$V_1 = V_2 = V_3 \qquad\qquad \text{Equation IV.4}$$

$$V_{total} = V_1 + V_2 + V_3 = \tfrac{1}{3} \cdot h_3 \cdot \pi \cdot r_3{}^2 \qquad\qquad \text{Equation IV.5}$$

$$\sin \alpha = \tfrac{r_3}{H} \qquad\qquad \text{Equation IV.6}$$

$$\cos \alpha = \tfrac{h_3}{H} \qquad\qquad \text{Equation IV.7}$$

$$\tan \alpha = \tfrac{\sin \alpha}{\cos \alpha} = \tfrac{r_3}{h_3} \qquad\qquad \text{Equation IV.8}$$

The ratio between r and h accordingly becomes:

$$\tan \alpha = \tfrac{r_1}{h_1} = \tfrac{r_2}{h_2} = \tfrac{r_3}{h_3} \qquad\qquad \text{Equation IV.9}$$

- Calculation h_1

$$V_1 = \tfrac{1}{3} \cdot V_{total}$$

Substituting V_1 and V_{total} in Equation IV.10 by Equations V.1 and V.5 respectively, resulted in:

$$\tfrac{1}{3} \cdot h_1 \cdot \pi \cdot r_1{}^2 = \tfrac{1}{3} \cdot \left(\tfrac{1}{3} \cdot h_3 \cdot \pi \cdot r_3{}^2 \right)$$

According to Equation IV.9, r_1 can be written as:

$$r_1 = \frac{h_1 \cdot r_3}{h_3}$$

Substitution of r_1 in Equation IV.11 by Equation IV.12 gives:

$$\tfrac{1}{3} \cdot h_1 \cdot \pi \cdot \left(\frac{h_1 \cdot r_3}{h_3} \right)^2 = \tfrac{1}{3} \cdot \left(\tfrac{1}{3} \cdot h_3 \cdot \pi \cdot r_3{}^2 \right)$$

From Equation IV.13, h_1 can be derived which results in Equation IV.14. First the brackets on the right hand side of the equal sign in Equation V.13 were eliminated and all h_1's were brought together:

$$\frac{1}{3} \cdot h_1^3 \cdot \pi \cdot r_3^2 \cdot h_3^{-2} = \frac{1}{3} \cdot \left(\frac{1}{3} \cdot h_3 \cdot \pi \cdot r_3^2 \right)$$

Subsequently, all terms which were present on the right hand side as well as on the left hand side of the equal sign were deleted:

$$h_1^3 \cdot h_3^{-2} = \frac{1}{3} \cdot h_3$$

Both sides were multiplied by $h_3{}^2$ in order to be able to move $h_3{}^{-2}$ from the left- to the right hand side of the equal sign:

$$h_1^3 = \frac{1}{3} \cdot h_3^3$$

After that, all terms were elevated to the power $^1/_3$, so the left hand side of the equal sign became h_1:

$$h_1^{3 \cdot \frac{1}{3}} = \left(\frac{1}{3} \right)^{\frac{1}{3}} \cdot h_3^{3 \cdot \frac{1}{3}}$$

$$h_1 = \left(\frac{1}{3} \right)^{\frac{1}{3}} \cdot h_3$$

- Calculation h_2

$$V_1 + V_2 = \tfrac{2}{3} \cdot V_{total}$$ Equation IV.15

Substituting V_1+V_2 by the first part (left hand side of the minus sign) of Equation IV.2 and V_{total} by Equation IV.5, resulted in:

$$\tfrac{1}{3} \cdot h_2 \cdot \pi \cdot r_2{}^2 = \tfrac{2}{3} \cdot \left(\tfrac{1}{3} \cdot h_3 \cdot \pi \cdot r_3{}^2 \right)$$ Equation IV.16

According to Equation IV.9, r_2 was written as:

$$r_2 = \tfrac{h_2 \cdot r_3}{h_3}$$ Equation IV.17

Substitution of r_2 in Equation IV.15 by Equation IV.16 resulted in:

$$\tfrac{1}{3} \cdot h_2 \cdot \pi \cdot \left(\tfrac{h_2 \cdot r_3}{h_3} \right)^2 = \tfrac{2}{3} \cdot \left(\tfrac{1}{3} \cdot h_3 \cdot \pi \cdot r_3{}^2 \right)$$ Equation IV.18

The same calculation steps as were used in order to transform Equation IV.13 into V.14 (Equations V.13a,b,c and d) were used to derive h_2 from Equation IV.18. Accordingly, h_2 became:

$$h_2 = \left(\tfrac{2}{3} \right)^{\tfrac{1}{3}} \cdot h_3$$ Equation IV.19

APPENDIX V. Spatial integration over the path

It was assumed that during diffuse light conditions, the sky has a uniform radiance resulting in an isotropic downward radiation. The contribution of an infinitesimally small portion of the sky to the irradiance at a point P of a horizontal surface can be explained as in Figure V.1 and Equation V.1.
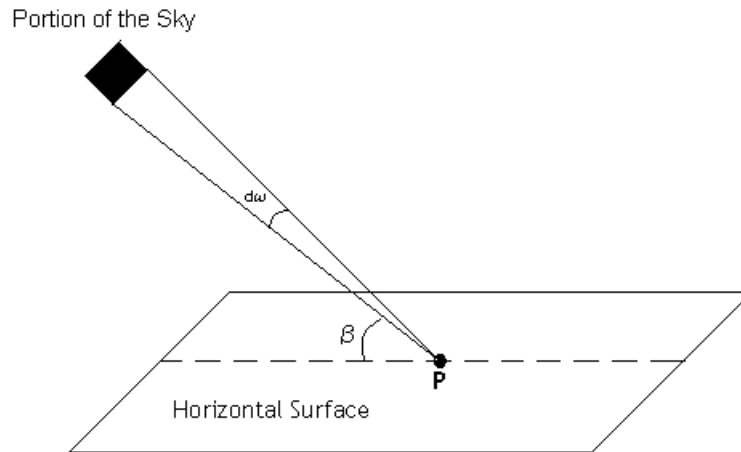
Figure V.1. Irradiance *S* on point P on the horizontal surface from a part of the sky with inclination *β*.

$$dS = N \, \sin \beta \, d\omega$$

Equation V.1

Where

N = radiance of the sky

$d\omega$ = infinitesimally small solid angle

β = inclination of the portion of the sky

dS depends on the radiance (N), on the height (angle β) of the sky portion above the surface and on the solid angle $d\omega$ of the radiation source. It is convenient to consider first a small solid angle bounded by the inclinations β and $\beta + d\beta$ in the vertical direction and by the azimuths α and $\alpha + d\alpha$ in the azimuthal (horizontal) direction. The entire sky dome can be thought of as being 'tiled' by such small pieces. The black square in Figure V.1 represents such a small 'tile'", of which the solid angle ($d\omega$) is given by:
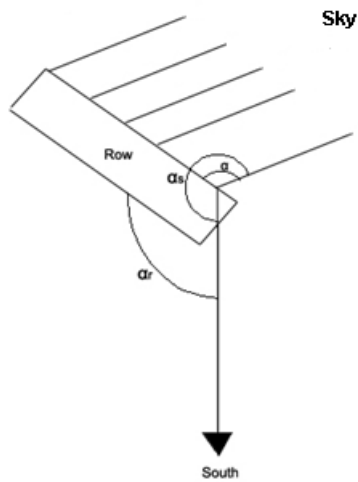
$$d\omega = \cos \beta \, d\beta \, d\alpha$$

Equation V.2

Substitution of $d\omega$ in Equation V.1 by Equation V.2 results in:

$$dS = N \, \sin \beta \, \cos \beta \, d\beta \, d\alpha$$

Equation V.3

Hereafter, the symbol α will be used for the difference between the azimuth of the sky portion and the azimuth of the plant row; $\alpha = \alpha_s - \alpha_r$ (Figure V.2).

Figure V.2. Difference between the azimuth of the sky portion (α_s) and the azimuth of the row (α_r), which results in α.

In order to facilitate the further calculations was switched to another coordinate system in the same plane as the incoming sun. This new coordinate system is depicted in Figure V.3, in which P represents a point on the upper hemisphere.
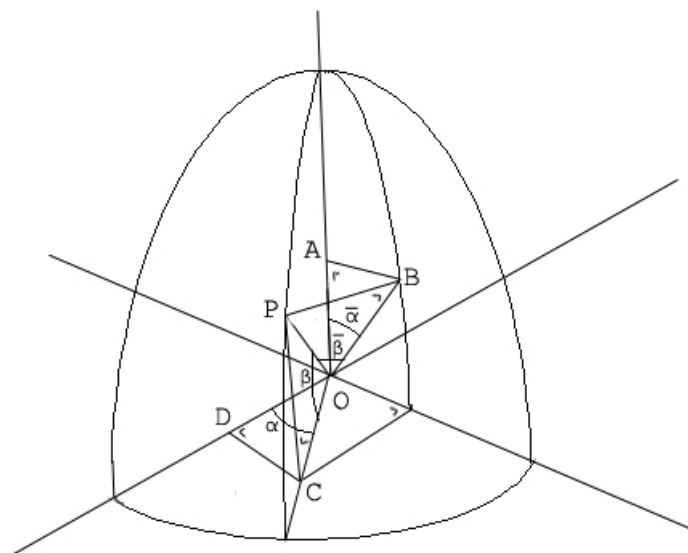
Figure V.3. Coordinate system in the plane of the incoming sun. P represents a point on the upper hemisphere, whereas α is the angle between the row and the sun with positive sign to the west (as explained above) and ß the inclination of the sun $\bar{\alpha}$ and $\bar{\beta}$ replace these respectively in this new coordinate system. Source: adapted from Goudriaan (1977).

As can be derived from Figure V.3, the relation between the new azimuth $\bar{\alpha}$ and inclination $\bar{\beta}$ are:

$$\sin\beta = \cos\bar{\alpha} \; \cos\bar{\beta}$$

Equation V.4

$$\sin\bar{\beta} = \cos\alpha \; \cos\beta$$

Equation V.5

Equation V.4 can be explained according to Figure V.3:

$$\sin\beta = \frac{PC}{OP}$$

Equation V.6

$$\cos\bar{\alpha} = \frac{OA}{OB}$$

Equation V.7

$$\cos\bar{\beta} = \frac{OB}{OP}$$

Equation V.8

Substituting $\sin\beta$, $\cos\bar{\alpha}$ and $\cos\bar{\beta}$ by Equations V.6, 7 and 8 respectively results in:

$\frac{PC}{OP} = \frac{OA}{OB} \cdot \frac{OB}{OP} = \frac{OA}{OP}$ and $OA = PC$ so $\frac{PC}{OP} = \frac{PC}{OP}$, which proves Equation V.4.

Also Equation IV.5 can be explained according to Figure V.3:

$$\sin\bar{\beta} = \frac{PB}{OP}$$

Equation V.12

$$\cos\alpha = \frac{OD}{OC}$$

Equation V.13

$$\cos\beta = \frac{OC}{OP}$$

Equation V.14

Substituting $\sin\bar{\beta}$, $\cos\alpha$ and $\cos\beta$ by Equations V.12,13 and 14 respectively, results in:

$\frac{PB}{OP} = \frac{OD}{OC} \cdot \frac{OC}{OP} = \frac{OD}{OP}$ and $PB = OD$, so $\frac{PB}{OP} = \frac{PB}{OP}$, which proves Equation V.5.

In Equation IV.3, the contribution to the irradiance of an infinitesimal surface ($\mathrm{d}S$) was given. This equation was integrated over the whole skydome; $-\pi/2$ till $\pi/2$ (Figure V.4) and angles α_1 and α_2 (Figure V.6), in order to calculate the total irradiance on a point in the path.
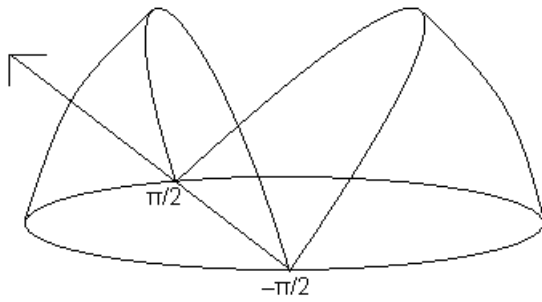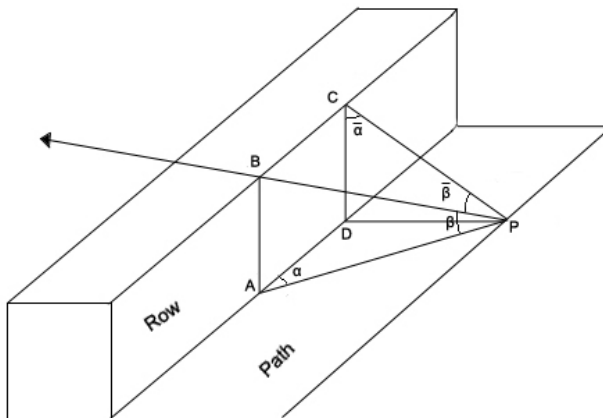
Figure V.4. Skydome from $-\pi/2$ to $\pi/2$. The arrow points in the direction of the plant row. Source: adapted from Pronk *et al.* (2003).

$$\int_{-\frac{\pi}{2}}^{\frac{\pi}{2}} \int_{\alpha_1}^{\alpha_2} N \cdot \sin \beta \cdot \cos \beta \; d\alpha \; d\beta$$

Equation V.15

Sin β was substituted by Equation V.4. Furthermore, *cos β* was substituted by $cos \; \bar{\beta}$ *since β*= $\bar{\beta}$ according to Figure V.5.

Figure V.5. Angles which the sunrays make with the row and the path in the orchard (after Gouderiaan, 1977).

$$\int_{-\frac{\pi}{2}}^{\frac{\pi}{2}} \int_{\alpha_1}^{\alpha_2} N \cdot \cos \bar{\alpha} \cdot \cos^2 \bar{\beta} \; d\bar{\alpha} \; d\bar{\beta}$$

Equation V.16

If the constants are placed outside the integral:

$$N \int_{\alpha_1}^{\alpha_2} \cos \bar{\alpha} \; d\bar{\alpha} \int_{-\frac{\pi}{2}}^{\frac{\pi}{2}} \cos^2 \bar{\beta} \; d\bar{\beta}$$

Equation V.17

Incorporating the standard formula $\cos^2 \bar{\beta} = \frac{1}{2} + \frac{1}{2} \cos 2\bar{\beta}$, which is true for all $\bar{\beta}$, results in the final integral:

$$N \int_{\alpha_1}^{\alpha_2} \cos \bar{\alpha} \; d\bar{\alpha} \int_{-\frac{\pi}{2}}^{\frac{\pi}{2}} \left(\tfrac{1}{2} + \tfrac{1}{2} \cos 2\bar{\beta}\right) d\bar{\beta}$$

Equation V.18

In order to integrate, the following integration rules were used:

$$\int \cos x \; dx = \sin x + c$$

Equation V.19

$$\int \cos 2x \; dx = \tfrac{1}{2} \sin 2x + c$$

Equation V.20

Which results in:

$$N \cdot [\sin \bar{\alpha}] \, |_{\bar{\alpha}_1}^{\bar{\alpha}_2} \cdot \left[\tfrac{\bar{\beta}}{2} + \tfrac{1}{4} \sin 2\bar{\beta}\right] |_{\frac{-\pi}{2}}^{\frac{\pi}{2}}$$

Equation V.21

The integral boundaries were filled in:

$$N \cdot (\sin \bar{\alpha}_2 - \sin \bar{\alpha}_1) \cdot (\tfrac{\pi}{4} + 0 + \tfrac{\pi}{4} - 0)$$

Equation V.22

$$N \cdot \tfrac{\pi}{2} \cdot (\sin \alpha_2 - \sin \alpha_1)$$

Equation V.23

In order to calculate irradiance relevant to the total irradiance (I), the above equation was diVded by πN. Since πN represents the total irradiance on a horizontal surface above the canopy.

$$I = \tfrac{1}{2} \cdot (\sin \bar{\alpha}_2 - \sin \bar{\alpha}_1)$$
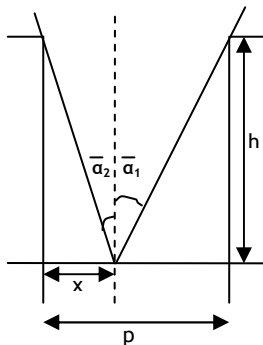
Equation V.24

Figure V.6. Representation of the incoming sun on a point in the path of the orchard (after Goudriaan, 1977). p=path and h=plant height.

The following equations were used according to Figure V.6:

$$\sin \bar{\alpha}_2 = \frac{x}{\sqrt{h^2 + x^2}}$$

Equation V.25

$$\sin \bar{\alpha}_1 = \frac{x - p}{\sqrt{h^2 + (p - x)^2}}$$

Equation V.26

Since $\bar{\alpha}_1$ was chosen to be negative, in the preVous equation x-p was used instead of p-x.

$\sin \bar{\alpha}_2$ and $\sin \bar{\alpha}_1$ in Equation V.24, were substituted by Equation V.25 and V.26:

$$= \int_{o}^{p} \left(\frac{1}{2} \frac{x}{\sqrt{h_r^2 + x^2}} - \frac{1}{2} \frac{x - p}{\sqrt{h_r^2 + (p - x)^2}}\right) dx$$

Equation V.27

In order to calculate the relative radiation onto the path (I_p) the equation above was diVded by p. Furthermore, the integral was split up and the boundaries filled in:

$$= \frac{\frac{1}{2}\int_0^P \frac{x}{\sqrt{h^2+x^2}}dx - \frac{1}{2}\int_0^P \frac{x-p}{\sqrt{h^2+(-p+x)^2}}dx}{p}$$

$$= \frac{\left[\frac{1}{2}\sqrt{h_r^2+x^2}\right]\Big|_0^P - \left[\frac{1}{2}\sqrt{h_r^2+(-p+x)^2}\right]\Big|_0^P}{p}$$

$$= \frac{\frac{1}{2}\sqrt{h^2+p^2} - \frac{1}{2}h - \frac{1}{2}h + \frac{1}{2}\sqrt{h^2+p^2}}{p}$$

Finally, the relative irradiance onto the path becomes:

$$I_p = \frac{\sqrt{h^2+p^2}-h}{p}$$

Equation V.28

APPENDIX VI. Additional results
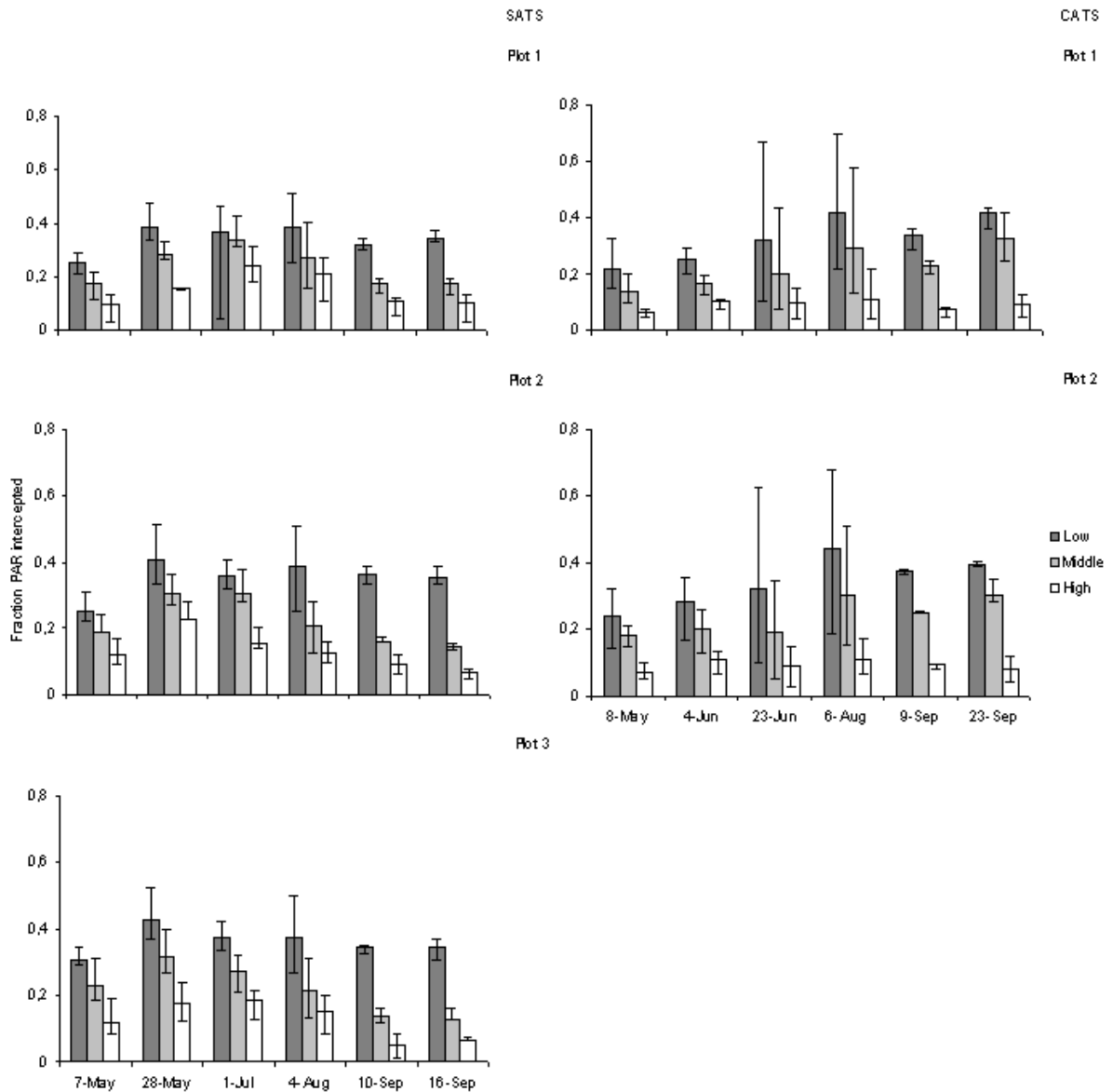
Figure VI.1. Fraction PAR intercepted by the spindle- (SATS) and columnar (CATS) apple tree systems per plot (average over the different measurement times on a day) from flowering till directly after harvest, depicted per apple tree system for the low, middle and high measurement heights. Measurements were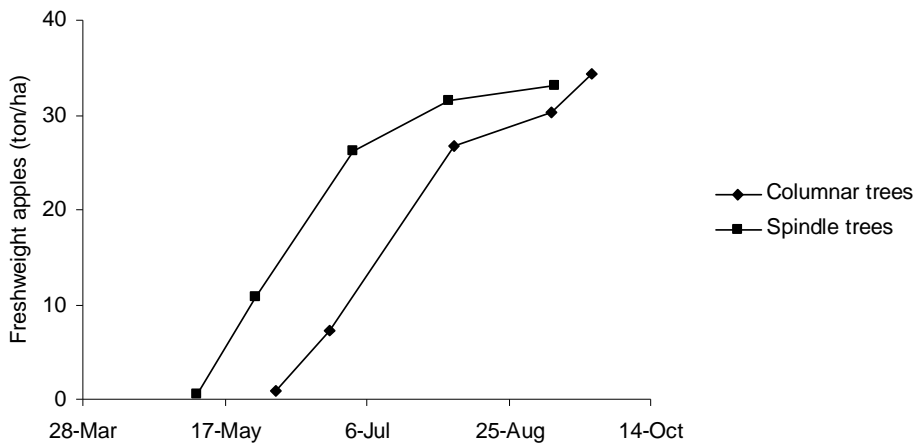 done approximately once a month (from flowering till right after harvest) three times during a day during diffuse-, and five times during a day during direct light conditions. Except for the third and the fourth measurements, which were done during homogeneous direct light conditions, the measurements were conducted during homogeneous diffuse light conditions. The ranges depict the highest and lowest fraction of PAR intercepted measured at each measurement time, describing the variability in PAR interception between the different measurement times during a day.

Figure VI.2. Fresh weight apple yield in ton/ha for the spindle- (SATS) and columnar (CATS) apple tree system, measured approximately once a month from about a month after flowering until harvest. Per measurement in time, the total number of apples present per plot were: 73, 88, 108, 97 and 62 for the SATS and 37, 33, 35, 35 and 28 for the CATS.
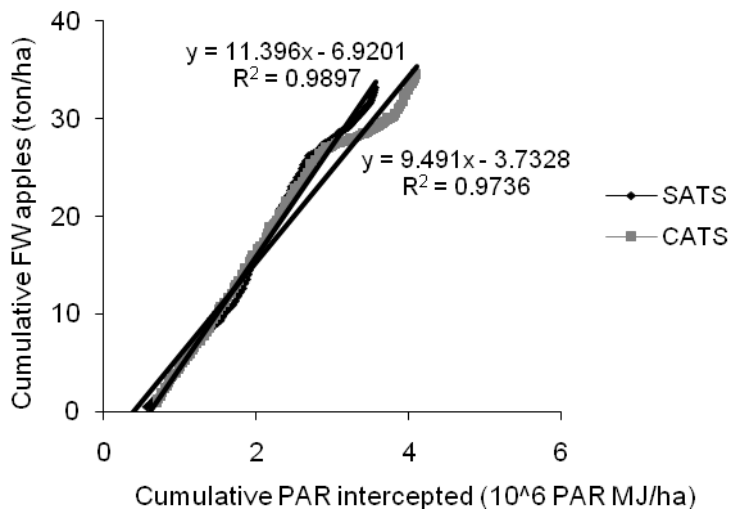
Figure VI.3. Relation between the cumulative amount of PAR intercepted (10^6 MJ PAR/ha) and the cumulative apple fresh weight (ton/ha) of the spindle- (SATS) and the columnar (CATS) apple tree system, if was assumed that the relation between the different PAR interception- and apple dry weight measurements over time is linear.

APPENDIX VII. ROWCROP

Table VII.1 Conversion of the abbreviations used in Chapter 2.3.1 (Theory light interception in row crop canopies) and the model ROWCROP.

Chapter 2.3.1	ROWCROP
h	H
p	P
r	W
LAI	L
k	k
LAI_{comp}	LP
$F_{i, comp}$	FO
F_i	FM
I_r	IW
I_p	IP
Sr_{ni}	SW
Sp_{ni}	SP
$F_{i, rowcrop}$	FCROP

Underneath the text of the FST-model ROWCROP can be found.

TITLE ROWCROPS SIMPLE
* written by Jan Goudriaan

* rows alternating with paths
* the rows are simplified to infinitely long rectangular blocks

* with height H and width W, separated by paths P
* the sky is simplified to a perfectly diffuse sky

* This model was used to calculate the fraction of PAR intercepted by the crop (FCROP)
* for columnar and spindle apple trees. Experimental gained information was used as input
* for the model: the extinction coefficient (PARAM K), the height of the trees (PARAM H),
* the width of the row (PARAM W), width of the path (PATH) and the leaf area index
(PARAM L).

TRANSLATION_GENERAL DRIVER='EUDRIV'

```
* Extinction coefficient:
PARAM K=


* Height of the plants:
PARAM H=


* Width W of the row and width PATH of the path:
PARAM W=    ;PATH=


PRINT FO,FM,FCROP,H,IW,IP,SO,SM,SW,SP,BALANC,CLUSTF


TIMER STTIME=0.;FINTIM=1.;DELT=1.;PRDEL=1.


* Leaf area index is used as independent variable:
PARAM L=


* Leaf area index L is always based on the total ground area


* LP is based on projected area:
LP=L*(W+PATH)/W


* if the plants were pushed together in monocultures,
* fraction of light absorbed FO and fraction light on the soil SO
FO=W/(W+PATH)*(1.-SO)
SO=EXP(-K*LP)


* if the leaves were spread out homogeneously
* fraction of light absorbed FM and fraction light on the soil SM
SM=EXP(-K*L)
FM=1.-SM


* in the actual arrangement, but with vertical black sheets at the
* sides of the rows and the leaves removed,
* the average light intensity at the soil surface under the row and
* on the path is found by analytical integration over the diffuse sky:
    IW=(SQRT(H*H+W*W)-H)/W
    IP=(SQRT(H*H+PATH*PATH)-H)/PATH


* SP and SW are radiation levels on the soil surface,
* in the path and in the row
```

* the actual light intensities on the soil are approximated as follows:
* SW under the row it is a weighted average of SO and SM
SW=IW*SO+(1.-IW)*SM

* SP on the path is larger than IP by a fraction transmitted through the rows:
SP=IP+(1.-IP)*SM

* FCROP is the approximation of the absorption by the crop
FCROP=(FO*(SP-SW) + FM*(1.-SO-SP+SW))/(1.-SO)

* CLUSTF is the effective cluster factor due to the row arrangement:
CLUSTF=FCROP/FM

* finally a check of the balance is calculated which ideally should be zero:
BALANC=FCROP+(SW*W+SP*PATH)/(W+PATH)-1.

END
STOP

APPENDIX VIII. Elasticity model parameters

Table 1. Elasticity of Fcrop to parameters h, p, w, k, and LAI at 10, 5, 2.5 and 1% deviation around the default value for the columnar apple tree system at the six measurement dates.

Parameters [2]	8-May	4-Jun	23-Jun	6 August	9-Sep	23-Sep
h 10%	0.10[1]	0.11	0.12	0.14	0.12	0.15
h 5%	0.10	0.11	0.12	0.14	0.12	0.15
h 2.5%	0.10	0.11	0.12	0.14	0.12	0.15
h 1%	0.10	0.11	0.12	0.14	0.12	0.15
p 10%	-0.11	-0.12	-0.14	-0.16	-0.14	-0.17
p 5%	-0.11	-0.12	-0.14	-0.16	-0.14	-0.17
p 2.5%	-0.11	-0.12	-0.14	-0.16	-0.14	-0.17
p 1%	-0.11	-0.12	-0.14	-0.16	-0.14	-0.17
w 10%	0.01	0.01	0.02	0.02	0.02	0.02
w 5%	0.01	0.01	0.02	0.02	0.02	0.02
w 2.5%	0.01	0.01	0.02	0.02	0.02	0.02
w 1%	0.01	0.01	0.02	0.02	0.02	0.02
k 10%	0.73	0.71	0.67	0.61	0.67	0.60
k 5%	0.73	0.71	0.67	0.61	0.67	0.60
k 2.5%	0.73	0.71	0.67	0.61	0.67	0.60
k 1%	0.73	0.71	0.67	0.61	0.67	0.60
LAI 10%	0.73	0.71	0.67	0.61	0.67	0.60
LAI 5%	0.73	0.71	0.67	0.61	0.67	0.60
LAI 2.5%	0.73	0.71	0.67	0.61	0.67	0.60
LAI 1%	0.73	0.71	0.67	0.61	0.67	0.60

[1] In Chapter 4.4.1 the calculation of the elasticity was explained.
[2] The % value behind the parameter name represents the deviation of the parameter around the default value.
[3] The abbreviations of the parameters are explained in Chapter 4 .

Table 2. Elasticity of Fcrop to parameters h, p, w, k, and LAI at 10, 5, 2.5 and 1% deviation around the default value for the spindle apple tree system at the six measurement dates.

Parameters [2]	7-May	28-May	1-Jul	4-Aug	10-Sep	16-Sep
h 10%	0.11[1]	0.14	0.14	0.15	0.12	0.12
h 5%	0.11	0.14	0.14	0.15	0.12	0.12
h 2.5%	0.11	0.14	0.14	0.15	0.12	0.12
h 1%	0.11	0.14	0.14	0.15	0.12	0.12
p 10%	-0.13	-0.18	-0.18	-0.18	-0.15	-0.15
p 5%	-0.13	-0.18	-0.18	-0.18	-0.15	-0.15
p 2.5%	-0.13	-0.18	-0.18	-0.18	-0.15	-0.15
p 1%	-0.13	-0.18	-0.18	-0.18	-0.15	-0.15
w 10%	0.02	0.03	0.03	0.04	0.03	0.03
w 5%	0.02	0.03	0.03	0.04	0.03	0.03
w 2.5%	0.02	0.03	0.03	0.04	0.03	0.03
w 1%	0.02	0.04	0.03	0.04	0.03	0.03
k 10%	0.72	0.62	0.61	0.60	0.67	0.68
k 5%	0.72	0.61	0.61	0.60	0.67	0.68
k 2.5%	0.72	0.62	0.61	0.60	0.67	0.67
k 1%	0.72	0.61	0.61	0.60	0.67	0.68
LAI 10%	0.72	0.62	0.61	0.60	0.67	0.68
LAI 5%	0.72	0.61	0.61	0.60	0.67	0.68
LAI 2.5%	0.72	0.62	0.61	0.60	0.67	0.68
LAI 1%	0.72	0.61	0.61	0.60	0.67	0.68

[1] In Chapter 4.4.1 the calculation of the elasticity was explained.
[2] The % value behind the parameter name represents the deviation of the parameter around the   default value.
[3] The abbreviations of the parameters are explained in Chapter 4 .